(U)

SECURITY CLASSIFICATION OF THIS PAGE

REPORT DOCUMENTATION PAGE

AD-A227 304

FILE COPY

a. REPORT SECURITY CLASSIFICATION
Unclassified

2a. SECURITY CLASSIFICATION AUTHORITY

SEP 2

2b. DECLASSIFICATION / DOWNGRADING SCHEDULE

OF REPORT

1. PERFORMING ORGANIZATION REPORT NUMBER(S)
ISI Report # 5877-01

5. MONITORING ORGANIZATION REPORT NUMBER(S)
AFOSR-TR- 90 0921

6a. NAME OF PERFORMING ORGANIZATION
Integrated Systems Inc.

6b. OFFICE SYMBOL (If applicable)

7a. NAME OF MONITORING ORGANIZATION
USAF, Air Force Office of Scientific Research

6c. ADDRESS (City, State, and ZIP Code)
2500 Mission College Blvd.
Santa Clara, CA 95054-1215

7b. ADDRESS (City, State, and ZIP Code)
Building 410
Bolling AFB, DC 20332-6448

8a. NAME OF FUNDING / SPONSORING ORGANIZATION
[redacted] AFOSR

8b. OFFICE SYMBOL (If applicable)
NA

9. PROCUREMENT INSTRUMENT IDENTIFICATION NUMBER
F49620-89-C-0043

8c. ADDRESS (City, State, and ZIP Code)
[redacted] Bolling AFB
Washington, DC 20332

10. SOURCE OF FUNDING NUMBERS

PROGRAM ELEMENT NO.	PROJECT NO.	TASK NO.	WORK UNIT ACCESSION NO.
61102F	2302	B1	

11. TITLE (Include Security Classification)
...aptive Control of Large Space Structures (U)

12. PERSONAL AUTHOR(S)
...obert L. Kosut

13a. TYPE OF REPORT	13b. TIME COVERED	14. DATE OF REPORT (Year, Month, Day)	15. PAGE COUNT
Final Report	FROM 2-1-89 TO 3-31-90	8-15-90	37

16. SUPPLEMENTARY NOTATION

17. COSATI CODES			18. SUBJECT TERMS (Continue on reverse if necessary and identify by block number)
FIELD	GROUP	SUB-GROUP	

19. ABSTRACT (Continue on reverse if necessary and identify by block number)

Preliminary results are presented for set estimation of uncertain nonlinear systems. Set estimation is a process in an adaptive robust control sytem which produces a set of models from the measured data. The set is then used in an on-line robust control design to implement a controller which is guaranteed to acheive performance goals for all members of the set. The scheme works whenever the actual system which produced the data is a member of the estimated set. The results in this report extend some previous work in linear set estimation to nonlinear systems. This report also summarizes an alaysis of an adaptive nonlinear system using the method of averaging.

20. DISTRIBUTION / AVAILABILITY OF ABSTRACT
☐ UNCLASSIFIED/UNLIMITED ☒ SAME AS RPT ☐ DTIC USERS

21. ABSTRACT SECURITY CLASSIFICATION
UNCLASSIFIED

22a. NAME OF RESPONSIBLE INDIVIDUAL
[redacted] Dr Spencer T. Wu

22b. TELEPHONE (Include Area Code)
[redacted] (202) 767-6962

22c. OFFICE SYMBOL
NA

DD FORM 1473, 84 MAR

83 APR edition may be used until exhausted.
All other editions are obsolete.

SECURITY CLASSIFICATION OF THIS PAGE
(U)

90 09 07 013

integrated systems inc.

Annual Technical Report
1 Feb 1989 through 31 Jan 1990

Adaptive Control of Large Space Structures

(Contract No. F49620-89-C-0043)

Prepared by:

Dr. Robert L. Kosut

Integrated Systems Inc.
2500 Mission College Boulevard
Santa Clara, California 95054-1215

Prepared for:

AFOSR, Directorate of Aerospace Sciences
Bolling Air Force Base
Washington, DC 20332

ISI Report No. 5877-01
15 Aug 1990

Contents

1 Background and Objectives

The Large Space Structure (LSS) research program was originally formulated in late 1982 in response to the increasing concern that performance robustness of Air Force LSS type systems would be inadequate to meet mission objectives principally because of uncertainties in both system dynamics and disturbance spectra. This lead to consideration of adaptive control systems, where disturbances and/or plant models are identified prior to or during control, thereby giving systems designers more options for minimizing the risk in achieving performance objectives.

In the early ACOSS and VCOSS programs issues of performance sensitivity, robustness, and achievement of very high performance in an LSS system were addressed. These programs established the need to accurately identify modal frequencies and mode shapes to acheive high-performance disturbance rejection for optical or RF systems, *e.g.* , [1]. For these cases, adaptive control mechanizations were shown to be needed to produce the three-to-five orders-of-magnitude reductions in line-of-sight jitter required by the mission.

The aim of adaptive control is to implement in real-time and on-line as many as possible of the design functions now performed off-line by the control engineer. Although it is easy to configure an adaptive system by connecting an estimator and control design rule, research is essential to identify the performance limitations of adaptive strategies for LSS control. The long range goal of this research program is to establish guidelines for selecting the appropriate strategy, to evaluate performance improvements over fixed-gain mechanizations, and to examine the architecture necessary to produce a practical hardware realization. The initial and continuing thrust, however, is to build a strong theoretical foundation without losing sight of the practical implementation issues.

2 Current Status

At the present time we stand at the beginning stages of the theoretical development in adaptive control. A summary of earlier efforts is contained in the recently published textbook *Stability of Adaptive Systems: Passivity and Averaging Analysis*, MIT Press. 1986. This publication is an outgrowth of research supported under this contract and involved a considerable amount of collaborative effort among several researchers in the field of adaptive control. The text discusses adaptive systems from the viewpoint of stability theory. The emphasis is on methodology and basic concepts, rather than on details of adaptive algorithm. The analysis reveals common properties including causes and mechanisms for instability and the means to counteract them. Conditions for stability are presented under slow adaptation, and the result is shown to be expressed as a frequency domain constraint on a mix of frequency respones and signal spectrum. These are greatly influenced by user choices regarding data filters and input spectrum. Some of the issues in the ideal case are explored in [13], a reprint of which is included in the Appendix of this report.

Under this contract we also explored the feasibility of applying the averaging analysis to the adaptive control of a nonlinear flexible system. We chose a Duffing type oscillator with a simple adaptive algorithm as a test case. The results were quite promising and have been reported in [18], a reprint of which is included in the Appendix of this report.

Another approach to adaptive control is to design on-line robust controllers from estimators which produce model sets, rather than a single model estimate usually produced by the estimator. This estimation problem, referred to as *set estimation* is the main topic of this report, and is also a topic of recent research activity.[1] Under AFOSR support, previous efforts along these lines have involved linear set estimation, *e.g.* , [15,16,17,19]. In this report we show how these methods can be extended to nonlinear flexible systems. Preliminary results are presented for flexible systems with uncertain memoryless nonlinearities at different locations.

In this report we discuss the "separation principal" between model set estimation and robust control design. This procedure allows for a more comprehensible approach to adaptive control design and differs from its predecessors in that model uncertainty is incorporated in the *synthesis* phase of the design rather than in the *anlysis* phase. By studying some typical example systems, the set estimation methodology is extended to the nonlinear case.

The results presented here for nonlinear systems, although of a preliminary and exploratory character, do indicate the feasibility of the basic approach as well as raising many new questions which need to be considered in future work, *e.g.* , what is the appropriate robust controller parametrization; how does it relate to model parametrization; how to iterate on the data if the estimate of model error is too large; what are the heuristics for experiment design. It is clear that concurrent effort is needed for both nonlinear set estimation and nonlinear robust control design - the former cannot be effective without the latter.

[1] Invited sessions have been organized by Dr. Kosut at the last three American Control Conferences (ACC) under the title, "System Identification for Control Design". A fourth is scheduled for the upcoming IEEE Conference on Decision and Control (CDC). In addition a mini-issue is being planned on this topic for the IEEE Transactions on Automatic Control. Dr. Kosut is one of the Guest Editors.

3 Design of Adaptive Control Systems

There are many ways to design or configure an adaptive control system. Figure 1 depicts the self-tuning-regulator (STR) configuration [3]. Two feedback processes make it adaptive, namely: (i) a model parameter estimator, and (ii) a control design rule.

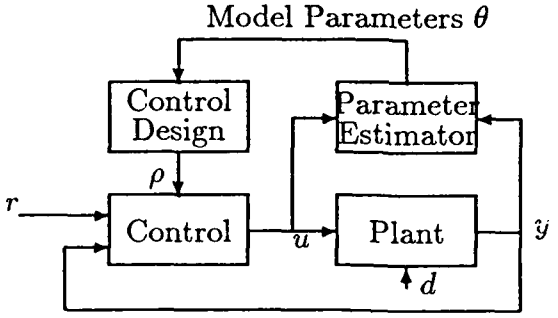

Figure 1: Self Tuning Regulator (STR).

The parameter estimator operates on the input-output data obtained from measurements (y, u) of the plant system and produces a model parameter estimate $\theta \in \mathbb{R}^p$. The parameter estimate is transformed by the control design rule into a controller parameter $\rho \in \mathbb{R}^\ell$, which is then used in a pre-determined parametric controller structure in feedback with the actual system.

It is obviously very easy to construct an adaptive system: just connect a control design rule and an estimator together. However, it is very difficult to insure that the resulting adaptive system will provide acceptable performance. This has been the goal of research in this area for over 30 years.

Roughly, if the true system is in the model set which underlies the parameter estimator, then the adaptive system will asymptotically reduce the error signal for arbitrary bounded exogenous inputs (r, d). Technically it is necessary that a a certain (closed-loop) transfer function is strictly-poitive-real (SPR) [23,11,2], *e.g.* , $H(s)$ is SPR if it is stable and satisfies,

$$\mathrm{Re}[H(j\omega)] \geq 0, \forall \omega \tag{1}$$

The main difficulty, to put it simply, is that the true system is *never* in the model set - there are always dynamical phenomena which remain unaccounted - and unfortunately, the SPR condition fails to hold. Moreover, the theory based on this property is sufficient and hence does not predict what will happen if the SPR condition is violated.

Under sufficiently slow adaptation the method of averaging can be applied to expose a mechanism for stability and instability [2],[27],[3]. This theory replaces the above SPR condition with a "signal dependent positivity condition" of the form,

$$R = \int \mathrm{Re}[H(j\omega)]S(\omega)\, d\omega > 0 \tag{2}$$

where $S(\omega) > 0$ is a spectral density matrix associated with the exogenous inputs. This condition is much less restrictive because even if $H(j\omega)$ fails to satisfy the SPR condition (1) at some frequencies, (2) can still hold provided the excitation is concentrated at those frequencies where $\mathrm{Re}[H(j\omega)] > 0$. Moreover, if any eigenvalue of R is negative then the system is unstable. In using the theory for design, the user must select an appropriate combination of data filtering and excitation spectrum. This task is similar to problems encountered in system identification [22] except that here the system being identified is in closed-loop, which vastly complicates the selction process.

To see this more clearly, consider the function $\Gamma(\theta)$ defined via Figure 2, *i.e.* , for every parameter choice θ there is a resulting parameter estimate denoted by the function $\Gamma(\theta)$.

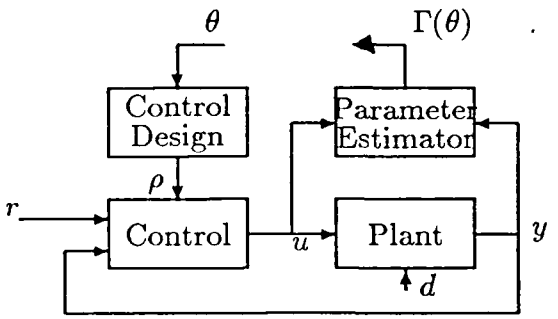

Figure 2: Illustration of the parameter map Γ.

It is shown in [24] that under slow adaptation, convergence points of the STR system in Figure 1 are precisely the fixed-points of Moreover, the fixed-point is stable if (2) holds and is unstable otherwise.

In summary, the averaging result shows that stability of the (nonlinear) adaptive system can be deduced from a frequency domain condition (2) which mixes signals and systems. However, there are some difficulties in utilizing the theory. In the first place, it is no trivial task to determine the fixed point(s) of the map Γ, *i.e.* , those $\theta \in \mathbb{R}^p$ satisfying $\theta = \Gamma(\theta)$. Secondly, both the transfer function $H(s)$ and the spectrum $S(\omega)$ depend in a complicated manner on the fixed-point and it is unclear how to precisely manipulate data filters and input spectrum to acheive either a satisfactory fixed-point and/or a satsfactory transient response in the adaptive parameter trajectory. To put it bluntly, the theory fails to produce a "user friendly" design method.

If we agree that the fundamantal difficulty in analyzing the adaptive system is the ubiquitous model uncertainty, then one alternate approach is to configure an adaptive control system which specifically accounts for the uncertainty. One such scheme, depicted in Figure 3, replaces the parameter estimator in Figure 1 with an estimator that produces a model set or set of uncertainty. This would avoid the major obstacle, namely, that the true system is not in the model set used for identification. This type of estimator is referred to as an *uncertainty estimator* or a *set estimator*. This differs from the estimator in the usual adaptive schemes (*cf.* Figure 1), where a *single* estimated model is produced, with

no information regarding its accuracy.

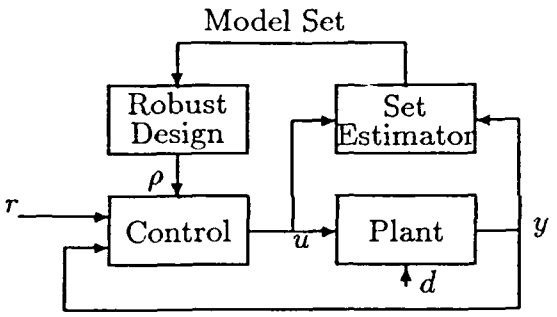

Figure 3: Adaptive control with uncertainty estimation.

The second change is to use a robust control design rule, *i.e.* , one that accepts a model set in the form produced by the set estimator. Under these conditions, if the true system which generated the measured data is contained in the estimated set, then the adaptive system is not only stable, but acheives the maximum performance possible given the estimated set of uncertainty.

Proceding in this way we have transformed the problem of adaptive control design from analysis with trial-and-error into separate synthesis problems in set estimation and robust control design. In effect this is a "separation principal" analogous to that in the LQG design.

Set estimators should at least have the following features:

- *Uncertain Parameters.* A capability to account for that part of the system which is known to be governed by physical laws or able to be described by known functions dependent on certain constant parameters. The parameters may only be known to lie within some range of variation.

- *Uncertain Dynamics.* Able to account for uncertain dynamics for which a parametric structure is not available or assumed, *e.g.* , neglected high frequency flexible modes, uncertain memoryless nonlinearities, *etc.*.

At present, methodologies for the design of set estimators are under development, *e.g.* , [30], [15], [21], [17],[10],[19], [31]. On the other hand, there is a reasonable maturity of methodologies for robust control design, particularly for plants with uncertain nonparametric linear dynamics, *e.g.* , [25], [32], [6,7], [9], [29]. Robust control design of plants with parametric uncertainty seems still underdeveloped despite some heroic efforts, *e.g.* , see [4,5] and the references therein.

In the remainder of the paper we principally address set estimation for linear and nonlinear systems. Section 2 provides a review of some recent results in linear set estimation and some new results in nonlinear set estimation. Section 3 provides a brief section on linear robust control of plants with both parametric and nonlinear uncertainty set descriptions.

4 Linear Set Estimation

Consider the linear-time-invariant model set:

$$\mathcal{G}(\Theta, W) = \{G_\theta(1 + \Delta W) : \theta \in \Theta,\ \|\Delta\|_\infty \leq 1\} \tag{3}$$

The set $\mathcal{G}(\Theta, W)$ describes both parametric and nonparametric uncertainty. The parametric uncertainty is reflected in the set $\{G_\theta : \theta \in \Theta\}$ where G_θ is a *parametric transfer function* with uncertain parameters $\theta \in \Theta \subset \mathbb{R}^p$. The mapping $\theta \rightarrow G_\theta$ is known but the exact parameter values are known only to be in some set Θ. The nonparametric uncertainty is reflected in the set $\{\Delta : \|\Delta\|_\infty \leq 1\}$. Thus Δ is an uncertain linear-time-invariant system only known to be stable and unity bounded in the $\mathcal{H}_\infty$-norm, which for continuous time systems is defined as $\|\Delta\|_\infty = \sup_{\omega \in \mathbb{R}} |\Delta(j\omega)|$ and for discrete time systems as $\|\Delta\|_\infty = \sup_{|\omega| \leq \pi} |\Delta(e^{j\omega})|$. W is a stable transfer function which reflects the size of the relative (or multiplicative) uncertainty, *i.e.* ,

$$\|\Delta\|_\infty = \|\frac{G - G_\theta}{G_\theta W}\|_\infty \leq 1$$

The above expression suggests interpreting the set $\mathcal{G}(\Theta, W)$ as a set of transfer functions "centered" at the parametric transfer function G_θ with a "radius of uncertainty" of $G_\theta W$.

It is usually possible in a modeling process to arrive at an initial parameter set Θ_0 and a weighting transfer function W_0. In the case when the prior set $\mathcal{G}(\Theta_0, W_0)$ is too coarse to lead to tolerable closed-loop performance levels, then a model set estimator is required to refine the prior information by making use of measured data. Specifically, we extract the following result from [19].

THEOREM

Suppose that the the measured data set

$$\{y, u : t = 1, \ldots, N\}$$

is obtained from the sampled-data system

$$y = Gu$$

where G has the discrete-time transfer function $G(z)$. Furthermore, suppose that from prior information

$$G \in \mathcal{G}(\Theta_0, W_0)$$

and the parametric transfer function in (3) has the structure:

$$\begin{aligned} G_\theta(z) &= \frac{B_\theta(z)}{A_\theta(z)} = \frac{b_1 z^{-1} + \cdots + b_m z^{-m}}{1 + a_1 z^{-1} + \cdots + a_n z^{-n}} \\ \theta^T &= [a_1 \cdots a_n\ b_1 \cdots b_m] \end{aligned}$$

Under these conditions, if G is initially at rest, and is either stable or in a stabilizing feedback, then:

$$G \in \mathcal{G}(\Theta_0, W_0) \cap \mathcal{G}(\Theta_N, W_0) \tag{4}$$

where Θ_N is the parameter set estimate,

$$\Theta_N = \{\theta : \|A_\theta y - B_\theta u\|_N \leq \|B_\theta W_0 u\|_N\} \tag{5}$$

with the N-point signal norm $\|x\|_N^2 = \sum_{t=1}^N x(t)^2$.

The above result implies that if the true parametric transfer function is $G_{\theta_{\text{true}}}$, where $\theta_{\text{true}} \in \mathbb{R}^p$ is the true parameter value, then

$$\theta_{\text{true}} \in \Theta_0 \cap \Theta_N$$

A good data set would insure that the new set estimate is strictly inside the prior estimate, that is

$$\Theta_0 \cap \Theta_N \subset \Theta_0$$

Since both A_θ and B_θ are affine functions of θ, it can be shown [19] that Θ_N describes either an ellipsoid or an hyperboloid in $\mathbb{R}^p$, depending on the data. Moreover, although the set $\Theta_0 \cap \Theta_N$ is not an ellipsoid, nonetheless a bounding ellipsoid can be obtained.

A similar result is obtained in [31] for a co-prime factor nonparametric uncertainty structure rather than the multiplicative one used here. More on bounding ellipsoids can be found in [8] who considered the problem of parameter set estimation with bounded noise and no unmodeled dynamics.

5 Nonlinear Set Estimation

The preceding principals of set estimation for linear-time-invariant systems can be applied to the set estimation of nonlinear systems. We will illustrate the problems using the following three example systems: (i) an input nonlinearity, (ii) an output nonlinearity, and (iii) a mechanical system with backlash.

5..1 Example 1: Input Nonlinearity

Consider the system shown in Figure 4 and described by:

$$y = G_\theta \bar{u}, \quad \bar{u} = f(u) \tag{6}$$

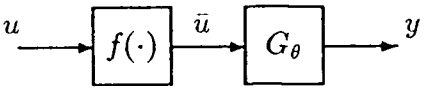

Figure 4: Input nonlinearity.

Make the following assumptions:

1. The function $f(\cdot)$ is a memoryless time-invariant nonlinearity known to lie in the sector
$$|f(u) - ku| \leq \delta|u|, \quad \forall |u| \leq \rho \tag{7}$$
where $\delta < k$ and $\rho > 0$ are known constants.

2. G_θ is a continuous-time linear-time-invariant system with stable transfer function $G_\theta(s)$ and where $\theta \in \mathbb{R}^p$ are uncertain parameters.

3. The measured data set is
$$\{y(t), u(t) \ : \ t = 1, \ldots, N\}$$
where the time t is normalized to the sampling interval.

The constants (k, δ, ρ) quantify the uncertainty in the nonlinear function $f(\cdot)$ in much the same way that W bounds the uncertain linear-time-invariant nonparametric dynamics in the previous section. A problem here, though, is that $\bar{u}$, the input to the linear part of the system , is not a measured variable. Moreover, the nonlinear function precludes describing any discrete-time transfer function from u into y. However, provided $f(\cdot)$ is sufficiently smooth, for fast sampling we have the following sampled-data approximation

$$y \approx G_\theta \bar{u}, \quad \bar{u} = f(u) \tag{8}$$

where now $G_\theta(s)$ is approximated by the zero-order-hold z-transform

$$G_\theta(z) = (1 - z^{-1})\mathcal{Z}\{\frac{1}{s}G_\theta(s)\}$$

This approximation is only valid at the sample times $t \in \{1, \ldots, N\}$. For example, if $f(\cdot)$ is a polynomial or rational function, then there certainly exists a (not necessarily small) region $|u| \leq \rho$ such that (7) holds.

To illustrate the problems in obtaining a set estimator even for the approximate system (8), suppose that (k, δ, ρ) are known, and we wish to estimate a parametric model for $G_\theta(z)$. For illustrative purposes, suppose that $G_\theta(z)$ is in the two-parameter set:

$$G_\theta(z) = \frac{B_\theta(z)}{A_\theta(z)} = \frac{bz^{-1}}{1 + az^{-1}}, \quad \theta = \begin{bmatrix} a \\ b \end{bmatrix} \tag{9}$$

After some algebra one obtains the following equivalent input/output description of (8):

$$A_\theta y - B_\theta u = B_\theta e \tag{10}$$

where $e(t)$ is an uncertain sequence satisfying

$$|e(t)| \leq \frac{\delta}{k}|u(t)|, \quad \forall t = 1, \ldots, N \tag{11}$$

Since (k, δ, ρ) are known and $u(t)$ is measured, the upper bound on the error sequence is known at each time instant. Combining the above expressions with prior information $\theta \in \Theta_0$, we obtain the parameter set estimate

$$\Theta_0 \cap \Theta_N$$

where Θ_N consist of those θ satisfying,

$$|y(t) + ay(t-1) - bu(t-1)| \leq \frac{\delta}{k}|bu(t-1)|, \tag{12}$$

for all $t = 1, \ldots, N$.

5..2 Example 2: Output Nonlinearity

In the above example, the nonlinearity was on the input. Now consider the case where the nonlinearity is on the output (see Figure 5) where

$$y = f(\bar{y}), \quad \bar{y} = G_\theta u \tag{13}$$

Proceeding as before we now have,

$$A_\theta y - B_\theta u = A_\theta e \tag{14}$$

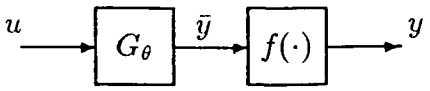

Figure 5: Input nonlinearity.

where now $e(t)$ is an uncertain sequence satisfying

$$|e(t)| \leq \frac{\delta}{k-\delta}|y(t)|, \quad \forall t = 1, \ldots, N \tag{15}$$

In this case the set estimate Θ_N consists of those θ satisfying,

$$|y(t) + ay(t-1) - bu(t-1)| \leq \frac{\delta}{k-\delta}\left(|y(t)| + |ay(t-1)|\right), \tag{16}$$

for all $t = 1, \ldots, N$.

5..3 Example 3: Mechanical System

Consider the mechanical configuration depicted in Figure 6.

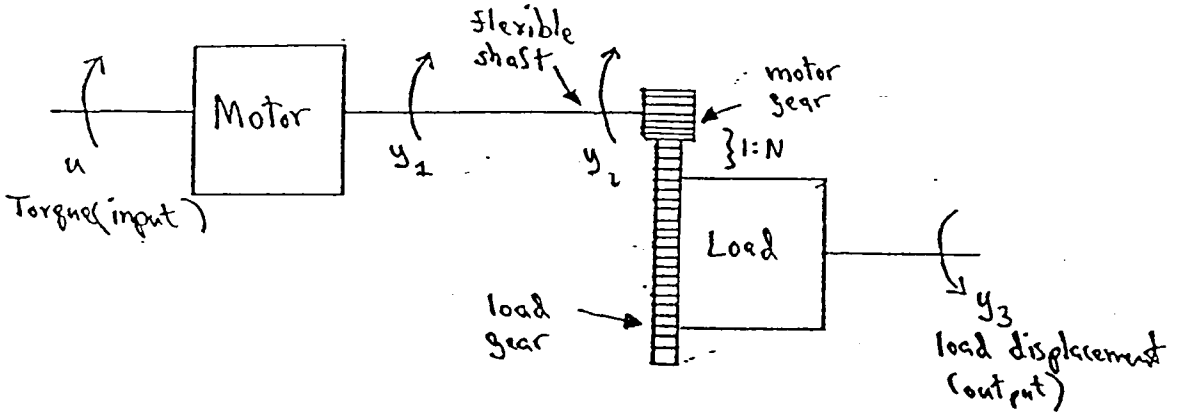

Figure 6: A flexible rotating system with backlash in the gear-train.

This system represents the case where tortional actuation is applied to a load through a flexible gear-train. The gearing is shown to occur at the end of the flexible member, although other combinations are certainly possible.

Neglecting any electronic dynamics, and assuming that the flexible rod is both uniform and damped, the motion of the rigid body and first tortional "mode" for small angular

deflections can be approximated by the system of differential equations,

$$\begin{aligned} J_M\ddot{y}_1 &= u + D(\dot{y}_2 - \dot{y}_1) + K(y_2 - y_1) \\ J_G\ddot{y}_2 &= -\bar{u} - D(\dot{y}_2 - \dot{y}_1) - K(y_2 - y_1) \\ J_L\ddot{y}_3 &= N\bar{u} \\ \bar{y} &= y_2 - Ny_3 \\ \bar{u} &= f(\bar{y}) \end{aligned}$$

where u denotes the input applied torque, (y_1, y_2, y_3) are angular deflections as indicated in the figure, $\bar{y}$ is the relative gear angle, and $f(\cdot)$ is a memoryless nonlinearity arising from backlash in the gear train. The constants are defined as follows: J_M, J_G, and J_L are the motor, motor gear, and load inertias, respectively, N is the gear ratio which is greator than one, and D, K are the damping and stiffness, respectively, of the elastic rod. The backlash nonlinearity $f(\cdot)$ has the typical shape as shown in Figure 7.

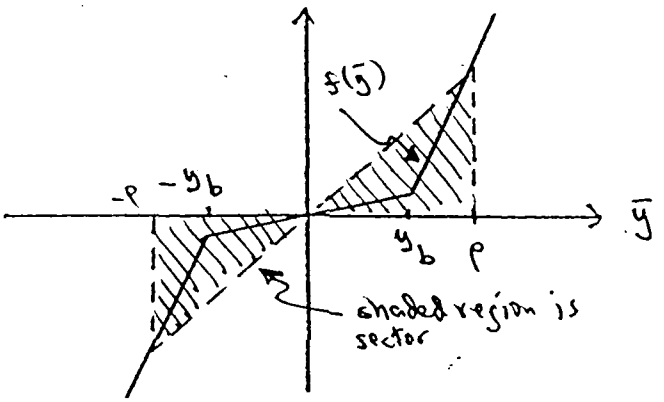

Figure 7: A typical backlash function.

The break-point parameter y_b relates to gear teeth spacing and the slopes in the two regions relate to gear teeth shapes. Typically for $|z| > y_b$ the slope is very large whereas for $|z| < y_b$ the slope is very small. It is clear that for some positive constants (k, δ, ρ) that $f(\cdot)$ satisfies the sector condition (7).

To illustrate how to compute a set estimate for the parameters of the mechanical system, suppose that the measured variables are

$$y = \begin{bmatrix} y_1 \\ y_3 \end{bmatrix}$$

and that (K, D) are uncertain parameters, *i.e.* ,

$$\theta = \begin{bmatrix} K \\ D \end{bmatrix}$$

Observe that the input to the nonlinear function is

$$\bar{u} = \frac{J_L}{N}\ddot{y}_3$$

One approach to describing a model set for this type of system is to approximate either the input or output to the nonlinear function. This would be like the ideal situations in the preceding two example systems. In this case, since y_3 is available as a measurement, the acceleration $\ddot{y}_3$ can be approximated by high pass filtering the measured output y_3. For example, let

$$\widehat{\ddot{y}_3} = Fy_3, \quad F(s) = \left(\frac{s}{s\tau + 1}\right)^2$$

where $1/\tau$ is sufficiently large so as to capture the dominant harmonics in the acceleration. Then,

$$\bar{u} \approx \hat{u} = \frac{J_L}{N}\widehat{\ddot{y}_3}$$

With this approximation the situation is very similar to the example where the nonlinearity is on the output. However, there is one difference: here the input to the nonlinear function also contains a term do to $\bar{u}$, which can also be approximated by $\hat{u}$. Thus, the appropriate model can be described by the *feedback system* shown in Figure 8.

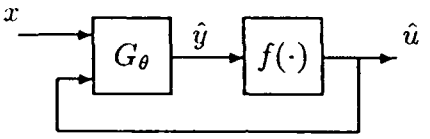

Figure 8: Feedback nonlinearity.

The system is described by,

$$\hat{u} = f(\hat{y}), \quad \hat{y} = G_\theta \begin{bmatrix} x \\ \hat{u} \end{bmatrix}, \quad x = \begin{bmatrix} y \\ u \end{bmatrix} \tag{17}$$

After some algebra, we obtain,

$$\bar{y} \approx \hat{y} = -\frac{J_M\hat{u} + J_G u}{A_\theta} + y_1 - Ny_3$$

where

$$A_\theta(s) = J_M J_G s^2 + (J_M + J_G)(Ds + K)$$

The procedure described in Example 1 can now be applied to obtain a set estimate which will contain the true parameters. Of course the precise conditions under which the true parameters are in the set estimate involve various approximations. In particular, due consideration must be given to approximating $\bar{u}$ by $\hat{u}$.

5.1 Standard Model Structure

Even though the three example systems are fairly general, it is also important to point out that they do not exhaust all the myriad possibilities. A very general model format, or template, is characterized in Figure 9.

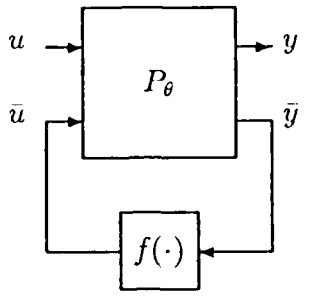

Figure 9: Standard model

This model form is discussed in detail in [20]. Here we make the following assumptions:

1. P_θ is a transfer matrix which depends on a parameter $\theta \in \mathbb{R}^p$ and which has the block structure:

$$\begin{bmatrix} y \\ \bar{y} \end{bmatrix} = \begin{bmatrix} P_{11} & P_{12} \\ P_{21} & P_{22} \end{bmatrix} \begin{bmatrix} u \\ \bar{u} \end{bmatrix} \tag{18}$$

2. $f(\cdot)$ is a scalar memoryless nonlinearity in the sector,

$$\alpha z \leq f(z) \leq \beta z, \quad \forall |z| \leq \rho$$

where $0 < \alpha < \beta$.

3. The measured data set is

$$\{y(t), u(t) \ : \ t = 1, \ldots, N\}$$

The standard form allows for scalar memoryless sector bounded nonlinearties, but the measured signals (y, u) can be vectors. Disturbances as well as nonparametric dynamic uncertainties can also be included by replacing the "feedback" with a more complicated system and by adding another input.

For the three example systems f is in the sector,

$$(k - \delta)u \leq f(u) \leq (k + \delta)u, \quad \forall |u| \leq \rho$$

where $\delta < k$.

For the system in Example 1 (8),

$$P_\theta = \begin{bmatrix} 0 & G_\theta \\ 1 & 0 \end{bmatrix}$$

For the system in Example 2 (10),

$$P_\theta = \begin{bmatrix} 0 & 1 \\ G_\theta & 0 \end{bmatrix}$$

And, for the system in Example 3 the transfer matrix P_θ has the block structure (18) with:

$$\begin{aligned} P_{11} &= \frac{Ds+K}{s^2[J_M J_G s^2 + (J_M+J_G)(Ds+K)]} \\ P_{12} &= \frac{N}{s^2 J_L} \\ P_{21} &= \frac{Ds+K}{s^2[J_M J_G s^2 + (J_M+J_G)(Ds+K)]} \\ P_{22} &= -\frac{N^2}{s^2 J_L} - \frac{J_M s^2 + Ds + K}{s^2[J_M J_G s^2 + (J_M+J_G)(Ds+K)]} \end{aligned}$$

In Example 3 we used the feedback approximation (17) which yields

$$P_\theta = \begin{bmatrix} 0 & I \\ G_{\theta,1} & G_{\theta,2} \end{bmatrix}$$

where G_θ in (17) has the block structure

$$G_\theta = [G_{\theta,1} \quad G_{\theta,2}]$$

These examples demonstrate that a very large class of mechanical systems can be captured by the standard form of Figure 9.

When P_{12}^{-1} exists, the input and output to the nonlinear function is given by:

$$\bar{y}_\theta = P_{21}u + P_{22}P_{12}^{-1}(y - P_{11}u) \tag{19}$$

$$\bar{u}_\theta = P_{12}^{-1}(y - P_{11}u) \tag{20}$$

We have explicitly used the θ subscript to indicate the parameter dependence. Thus, the parameter set estimate follows directly from the sector condition as,

$$\Theta_N = \{\theta \ : \ \alpha\bar{u}_\theta(t) \le \bar{y}_\theta(t) \le \beta\bar{u}_\theta(t), \ \ \forall t = 1, \ldots, N\} \tag{21}$$

Observe also that in the case when (u, y) are vector signals, the above will still hold if P_{12}^{-1} is replaced with the pseudo-inverse

$$P_{12}^{\dagger} = (P_{12}^T P_{12})^{-1} P_{12}^T$$

The standard model structure (Figure 9) can also handle multiple sector nonlinearities by replacing $f(\cdot)$ with a diagonal matrix nonlinearity

$$\bar{u} = F(\bar{y}) = \text{diag}[f_1(\bar{y}_1) \cdots f_p(\bar{y}_p)]$$

where $(\bar{u}, \bar{y})$ are now vector quantities. The sector conditions can now apply to each of the diagonal entries.

5.2 Disturbance Modeling

To make the model sets more realistic it is necessary to account for disturbances. For example, consider (8) with an additional disturbance term $d(t)$,

$$y = G_\theta \bar{u} + d, \qquad \bar{u} = f(u)$$

With $G_\theta = B_\theta / A_\theta$ we now obtain,

$$A_\theta y - B_\theta u = B_\theta e + A_\theta d \tag{22}$$

where $e(t)$ satsifies (11)

$$|e(t)| \leq = \frac{\delta}{k}|u(t)|, \quad \forall t = 1, \ldots, N$$

Suppose that $d(t)$ is unknown but bounded by,

$$|d(t)| \leq d_m, \quad \forall t = 1, \ldots, N \tag{23}$$

In effect both $e(t)$ and $d(t)$ have known bounds and by analogy with the preceding example we can easily construct (in principal) the corresponding set estimates.

It is obvious though that there are many forms for how a disturbance can influence a particular system. This leads to considering the standard model with an additional disturbance input as shown in Figure 10.

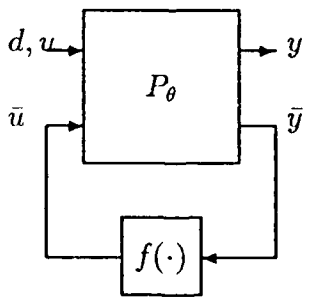

Figure 10: Standard model with disturbance.

5.3 Nonparametric Uncertainty

A more versatile model set would not only include disturbances and sector nonlinearities, but also uncertain nonparametric linear-time-invariant dynamics. For example, consider the system described by:

$$y = G_\theta(1 + \Delta W)\bar{u} + d, \qquad \bar{u} = f(u) \tag{24}$$

where $f(\cdot)$ is a sector nonlinearity, $d(t)$ is a bounded disturbance, Δ is an uncertain transfer function which satisfies $\|\Delta\|_\infty \leq 1$, and W is a known stable transfer function.

Now, reconfigure the system into a "structured" standard form as in [7,26] shown below in Figure 11.

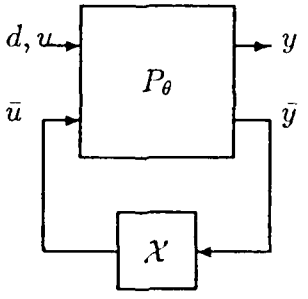

Figure 11: Standard model with disturbance and uncertainty.

Here the "feedback" matrix operator $\mathcal{X}$ contains all the model uncertainty,

$$\mathcal{X} = \begin{bmatrix} f(\cdot) & 0 \\ 0 & \Delta \end{bmatrix}$$

It is the diagonal structure of this matrix operator which causes difficulties in computing an optimal model set.

6 Robust Control Design

6.1 Robust Nonlinear Control

There are some well developed approaches to nonlinear control design. For example, there are the classical methods of gain scheduling, analysis via harmonic balancing (describing function analysis), and the method of feedback linearization. This latter approach is effectively a generalized gain scheduling procedure. In fact it is a true synthesis method, that is, a nonlinear control is directly designed from the nonlinear model [14]. The basic idea is to apply a nonlinear feedback which brings the closed-loop system into a purely linear form, which has obvious advantages for control design. A difficulty with the method is that the linearizing feedback requires an exact knowledge of the type of system nonlinearities. Moreover, the control is typically much more complex than a gain schedule, which bothers many design engineers. However, one can argue that feedback linearization can give the designer a means to evaluate the limits of achievable performance from a feedback system. Robustness of feedback linearization to model errors is an open area in basic research. Some work on robustness to uncertian nonlinearities has been advanced in the robotics area, where feedback linearization is there referred to as "computed torque", [28]. Developing robust nonlinear control is an area for some future work. To gain some insight into the issues we consider next the case of robust linear control of an uncertain nonlinear system.

6.2 Robust Linear Control of Nonlinear Model Sets

The premise is that the uncertainties are described via prior information on the nonlinear sector and a set estimator which describes the range of uncertain parameters in the linear-time-invariant part of the system.

As an illustrative example, consider the uncertain nonlinear plant with a linear feedback control,

$$y = d + f(\bar{y}), \quad \bar{y} = G_\theta u, \quad u = -Ky \tag{25}$$

where G_θ and K are linear-time-invariant systems, K is the linear feedback controller, $f(\cdot)$ is a memoryless nonlinearity, y is the measured output to be controlled, and d is a disturbance as seen at the output. The control objective is to attenuate the effect of the disturbance at the output despite the uncertainties in the system model. Specifically, the system uncertainties are as follows:

- the nonlinear function $f(\cdot)$ is in the sector,

$$|f(\bar{y}) - \bar{y}| \leq \delta|\bar{y}|, \quad \forall|\bar{y}| \leq \rho$$

- the parameters in the linear-time-invariant system G_θ are in the set $\hat{\Theta}$.

Observe that these uncertainty sets can arise from a combination of set estimation and/or prior information. From the control design viewpoint the source of the uncertainty is not relavent.

To analyze this system we make the following convenient defintions:

$$\begin{aligned} \Delta(\bar{y}) &= f(\bar{y}) - \bar{y} \\ S_\theta &= (1 + G_\theta K)^{-1} \\ T_\theta &= G_\theta K(1 + G_\theta K)^{-1} = 1 - S_\theta \end{aligned}$$

Observe that $\Delta(\cdot)$ satisfies the sector condition

$$|\Delta(\bar{y})| \leq \delta|\bar{y}|, \quad \forall|\bar{y}| \leq \rho$$

The transfer functions (S_θ, T_θ) are the closed-loop transfer functions from disturbance d to output y and control u, respectively, if the nonlinear function $f(\cdot)$ is replaced by the identity operator, which in this case is the "nominal" nonlinearity. The nonlinear feedback system is then equivalently expressed as:

$$\begin{aligned} y &= S_\theta(d + \varepsilon) \\ \varepsilon &= \Delta(\bar{y}) \\ \bar{y} &= -T_\theta(d + \varepsilon) \end{aligned}$$

Now, let $T_\theta(t)$ denote the impulse response of $T_\theta(s)$, and suppose that there are constants $M \geq 1$, $\alpha > 0$, and $r > 0$, independent of θ, such that for all $t \geq 0$,

$$\begin{aligned} |T_\theta(t)| &\leq Me^{-\alpha t} \\ |(T_\theta d)(t)| &\leq r \end{aligned}$$

Application of the Bellman inequality [12] yields:

$$|\varepsilon(t)| \leq \frac{\delta r}{1 - \delta M/a}$$

provided that

$$\begin{aligned} \delta &< \frac{a}{M} \\ r &< (1 - \delta M/a)\,\rho \end{aligned}$$

The above inequalities bound $\varepsilon(t)$, which appears as an additional disturbance. Thus, the ideal closed-loop transfer functions (S_θ, T_θ) must be shaped to make $\varepsilon(t)$ small. In addition, the linear controller K has other goals *e.g.* ,to robustly stabilize the linear-time-invariant model set $\{G_\theta : \theta \in \hat{\Theta}\}$.

References

[1] *Active Control of Space Structures (ACOSS)*, Phase 1a Final Report prepared by LMSC and ISI for Darpa under contract F30602-80-C-0087, Aug. 1981.

[2] B.D.O. Anderson, R.R. Bitmead, C.R. Johnson, Jr., P.V. Kokotovic, R.L. Kosut, I.M.Y. Mareels, L. Praly, and B.D. Riedle, *Stability of Adaptive Systems: Passivity and Averaging Analysis*, MIT Press, 1986.

[3] K.J. Åström and B. Wittenmark, *Adaptive Control*, Addison-Wesley, 1989.

[4] B.R. Barmish, "New tools for robustness analysis," *Proc. 27th IEEE CDC*, Austin, TX, 1988.

[5] R. Biernacki, H. Hwang, and S.P. Bhattacharyya, "Robust stability with structured real parameter perturbations," *IEEE Trans. Automat. Contr.*, vol. AC-32, no. 6, pp.495-506, June 1987.

[6] J.C. Doyle and G. Stein, "Multivariable Feedback Design: Concepts for a Classical/Modern Synthesis," *IEEE Trans. Automat. Contr.,* Feb. 1981.

[7] J.C. Doyle, J.E. Wall, and G. Stein, "Performance and robustness analysis for structured uncertianties," *Proc. IEEE CDC*, pp.629-636, 1982.

[8] E. Fogel and Y.F. Huang, "On the value of information in systemm identification - bounded noise case," *Automatica*, vol. 18, pp.229-238, 1982.

[9] B.A. Francis and G. Zames, "On $\mathcal{H}_\infty$-optimal Sensitivity Theory for SISO Feedback Systems," *IEEE Trans. Automat. Contr.,* Vol. 29, pp. 9-16, 1984.

[10] G.C.Goodwin and M.E.Salgado,"Quantification of uncertainty in estimation using an embedding principle," *Proc. 1989 ACC*, Pittsburgh, PA, June 1989.

[11] G.C. Goodwin and K.S. Sin, *Adaptive Filtering, Prediction, and Control*, Prentice-Hall, New Jersey, 1984.

[12] J.K. Hale, *Ordinary Differential Equations*, Kreiger, Molaban, FL, 1980; originally published (1969), Wiley (Interscience), New York.

[13] F. Hansen, G.F. Franklin, and R.L. Kosut, "Closed-loop identification via the fractional representation: experiment design," *Proc. 1989 ACC*, Pittsburg, PA, June 21-23, 1989.

[14] A. Isidori and C. Byrnes, "Output regulation of nonlinear systems," *IEEE Trans. on Aut. Contr.*, Vol. AC-32, No. 2, pp.131-140, Feb. 1990.

[15] R.L. Kosut, "Adaptive Calibration: An Approach to Uncertainty Modeling and On-Line Robust Control Design", *Proc. 25th IEEE CDC*, Athens, Greece, Dec. 1986.

[16] R.L. Kosut, "Adaptive control of large space structures: uncertainty estimation and robust control calibration," *Large Space Structures: Dynamics and Control*, edited by S.N. Atluri and A.K. Amos Springer-Verlag, 1987.

[17] R.L. Kosut, "Adaptive Control via Parameter Set Estimation," *Int. Journal of Adapt. Contr. and Sig. Proc.*, vol. 2, pp.371-399, 1988.

[18] R.L. Kosut, D. Meldrum, and G.F. Franklin, "Adaptive control of a nonlinear oscillating system " *Proc. 1989 ACC*, Pittsburg, PA, June 21-23, 1989.

[19] R.L. Kosut, M. Lau, and S. Boyd, "Identification of Systems with Parametric and Nonparamtric Uncertainty," *Proc. 1990 ACC*, May, 1990, San Diego, CA.

[20] J.M. Krause and P.P Khargonekar, "Parameter identification in the presence of nonparametric dynamic uncertainty," *Automatica*, vol. 26, no. 1, pp.113-123, 1990.

[21] R. O. LaMaire, L. Valavani, M. Athans, and G. Stein , "A Frequency- Domain Estimator for Use in Adaptive Control Systems", *Proc. 1987 ACC*, pp 238-244, Minn., MN, June 1987.

[22] L. Ljung,, *System Identification: Theory for the User*, Prentice- Hall, NJ, 1987.

[23] K.S. Narendra, Y.H. Lin, and L. Valavani, "Stable Adaptive Control Design, Part II: Proof of Stability", *IEEE Trans. Auto. Control*, Vol. AC-25, No. 3, pp.440-449, 1980.

[24] S. Phillips and R.L. Kosut, "On computing the equilibrium of the averaged system for the self-tuning-regulator," *Proc. 1990 ACC*, pp.567-568, San Diego, CA, May, 1990.

[25] M.G. Safonov, A.L. Laub, and G.L. Hartmann, "Feedback Properties of Multivariable Systems: The Role and Use of The Return Difference Matrix", *IEEE Trans. Aut. Contr.*, vol AC-26, Feb. 1981.

[26] M. G. Safonov, "Stability margins of diagonally perturbed multivariable systems," *IEEE Proc.*, 129-D, pp.251-256, Nov. 1982.

[27] S. Sastry and M. Bodson, *Adaptive Control: Stability, Convergence, and Robustness*, Prentice-Hall, 1989.

[28] *IEEE Trans. on Aut. Contr.*, Vol. AC-33, No. 11, pp. 995-1003, Nov. 1988.

[29] M. Vidyasagar, *Control System Synthesis: A Factorization Approach*, MIT Press, Cambridge, MA, 1985.

[30] B. Wahlberg , "On Model Reduction in System Identification," *Proc. 1986 ACC*, pp. 1260-1266, Seattle, WA, June 1986.

[31] R.C. Younce and C.E. Rohrs, "Identification with nonparametric uncertainty," *Proc. ISCAS 1990*, New Orleans, LA, May 1-4,1990.

[32] G. Zames, "Feedback and Optimal Sensitivity: Model Reference Transformations, Multiplicative Seminorms and Approximate Inverses", *IEEE Trans. Auto. Contr.*, **AC-26:**301–320, April 1981.

A Appendix: Reprints of Technical Articles

Proc. 1989 ACC
Pittsburgh, PA
June 21-23, 1989

Adaptive Control of a Nonlinear Oscillating System

Robert L. Kosut* Deirdre Meldrum† Gene F. Franklin†

Abstract A slowly adapting feedforward controller is applied to a nonlinear (Duffing) oscillator. Simulation results show that the adaptation continues relentlessly to improve performance despite the complex system behavior, *i.e.* , the system state passes in and out of both chaotic and multi-periodic attractors, finally settling down to a "quiet" periodic orbit. An analysis is presented based on the method of averaging. Under slow parameter adjustment it is shown that the source of the complex behavior is the nonlineariy in the system being controlled, not that introduced by the adaptation.

1 Introduction

Adaptive control systems can be generically represented[1] by the set of coupled ordinary differential equations:

$$\dot{x} = g(t,x,\theta) \quad (1)$$
$$\dot{\theta} = \gamma f(t,x,\theta) \quad (2)$$

In (1), $x \in \mathbb{R}^n$ is referred to as the "state" and consists of dynamical states of the system being controlled, controller states, and filter states in the parameter estimator. The function $g(t,x,\theta)$ is determined by the system dynamics and the controller/estimator design. In (2), $\theta \in \mathbb{R}^p$ is the adaptive parameter whose rate of adjustment is governed by a scalar constant $\gamma > 0$, referred to as the adaptation gain, and a function $f(t,x,\theta)$ determined by the designer. Observe that when the parameters are held fixed, the system is governed by the nonlinear system (1) for constant parameter θ.

In the case of an adaptive *linear* system, (1)-(2) reduce to,

$$\dot{x} = A(\theta)x + B(\theta)w(t) \quad (3)$$
$$\dot{\theta} = \gamma f(t,x,\theta) \quad (4)$$

where $w(t) \in \mathbb{R}^m$ consists of all exogenous inputs such as references and disturbances, and $A(\theta) \in \mathbb{R}^{n\times n}$ and $B(\theta) \in \mathbb{R}^{n\times m}$ are matrix functions of the parameter θ, the specific f ons depending on the control design rule d the parameter estimation model set. In this case when the parameters are held fixed, the system is governed by the f system (3) with θ constant.

An adaptive control system, although a special type of nonlinear system, is nonetheless a nonlinear system, and as such one would expect to encounter limit cycles, bifurcations, and chaos. In the case of adaptive linear control (3)-(4) , these latter phenomena are known to occur as the adaptation speed is increased (large γ), *e.g.* , [Mareels and Bitmead(1986,1988)], [Salam and Bai(1988)], [Cyr *et al.*(1983)], [Riedle and Kokotovic(1984)], and [Ydstie(1986)]. Thus, *rapid* adaptation alone can induce bifurcating and chaotic behavior.

In this paper we explore the case of adaptively controlling a nonlinear system under *slow* adaptation (small γ). As we will see, chaotic phenomena will appear primarily because of nonlinearity in the system being controlled, and not because of adaptation. Specifically, we examine a Duffing system under feedforward model reference adaptive control with slow adaptation. A simulation study is performed along with an analysis using the method of averaging, which has proven to be very successful for slow adaptation of linear systems, *e.g.* , Anderson *et al.*(1986), Sastry and Bodson(1988), Åström and Wittenmark(1989).

2 Adaptive Duffing System

The system to be controlled is the Duffing system:

$$\ddot{x} + k\dot{x} + x^3 = u \quad (5)$$

where $k > 0$ is a small damping coefficient, x is a measured output, and u is the control input. Prior knowlege of the damping and cubic nonlinearity is assumed unavailable, and hence, we implement the adaptive control:

$$u = \theta r$$
$$\dot{\theta} = \gamma r(r - x) \quad (6)$$

The adaptive parameter is θ, a feedforward control gain, $\gamma > 0$ is the adaptation gain, and r is a reference command which is to be followed by the output x. This adaptation rule is an approximation of a so-called "gradient" rule where the rate of adjustment is proportional to the

*Integrated Systems Inc., 2500 Mission College Blvd., Santa Clara, CA 95054 and Information Systems Lab, Stanford University.
Research support from AFOSR Contract F49620-89-C-0043DEF and NSF Grant ECS-86-05646.
†Information Systems Laboratory, Stanford University, Stanford, CA 94305.

[1] Modulo implementation via a digital computer.

negative gradient, with respect to the parameter θ, of an instantaneous error function. In this case the exact gradient rule is

$$\dot{\theta} \sim -\frac{\partial}{\partial\theta}(x-r)^2 \sim \psi(r-x)$$

where ψ is the instantaneous gradient of x, that is, $\psi = \partial x/\partial\theta$. Thus, for constant θ, ψ satisfies the differential equation

$$\ddot{\psi} + k\psi + 3x^2\psi = r$$

Since ψ depends on the unknown damping and cubic nonlinearity in the system (5), the pure gradient rule $\dot{\theta} = \gamma\psi(r-x)$ cannot be implemented. Using the (crude but simple) approximation $\psi \approx r$ yields the algorithm of (6).

Before studying the adaptive system (5)-(6) , recall that the Duffing system (5) for *constant* θ has been extensively examined. In particular, Ueda [Ueda(1980)] made an exhaustive study with $u = B\cos t$ and tabulated the resulting long-term behavior as a function of the parameters (k, B). For example, with $(k, B) = (.08, .2)$, there are five coexisting periodic attractors, whereas for $(k, B) = (.05, 7.5)$, $(.25, 8.5)$, or $(.1, 12.)$, the attractors are all chaotic.[2]

As an example, for $(k, B) = (.05, 7.5)$, Figure 1(a) displays a plot of points of $\dot{x}(t)$ vs. $x(t)$ at 900 2π-periodic strobe times, *i.e.* , $t \in \{2\pi k : k = 1, \ldots 250(2\pi)\}$. Such a plot is referred to as a *Poincare' section*. Figure 1(b) shows a corresponding time history of $\dot{x}(t)$ vs. $x(t)$ for 50 periods of the reference $u = 7.5\cos t$, *i.e.* , $t \in [0, 50(2\pi)]$.

Given the quite complex behavior of the system (5) when θ is constant and r is a sinusoidal reference, it is to be expected that if θ is slowly adapted, then the system (5)-(6) will pass through regions which contain chaotic and/or multi-periodic attractors.

3 Simulation Results

Simulations of (5)-(6) using MATRIX$_X$ software were performed under the following conditions:

reference

$$r = A\cos t, \quad A = 0.1$$

damping

$$k = .05$$

adaptation gain

$$\gamma = \begin{cases} 0 & 0 \le t < 250(2\pi) \\ .01 & 250(2\pi) \le t < 750(2\pi) \\ .05 & 750(2\pi) \le t < 4250(2\pi) \end{cases}$$

initial conditions

$$(\theta, x, \dot{x}) = (75, 0, 0)$$

integration algorithm

4th-order Kutter-Merson integration algorithm with a fixed step-size equal to 1/200th of the period of the reference signal r, *i.e.*

$$T = 2\pi/200 \tag{7}$$

To initialize the system there is no adaptation ($\gamma = 0$) for the first 250 periods. This is followed by 500 periods of very slow adaptation ($\gamma = .01$), and then the remainder of the time at relatively slow adaptation ($\gamma = .05$). The adaptive gain, γ, was chosen to produce slow adaptation to prevent any possible bifurcations and chaos soley as a result of too rapid an adaptation, which, as previously mentioned, is known to occur in adaptive systems even when the system being controlled is linear. Thus, initially after the adaptation begins, $\theta r \approx 7.5\cos t$. Referring to Figure 1, the initial response of (5)-(6) will be chaotic. What we hope to see is that the adaptation brings the system to a more quiescent condition, which in fact is what occurs. Figures 2- 3 show the results of the simulation over 4250 periods of the reference, *i.e.* , for $0 \le t \le 4250(2\pi)$.

Figure 2(a) shows values of x and θ at the 1-period strobe times $t \in \{2\pi k : k = 1, \ldots, 4250\}$. Figure 2(b) shows the (x, θ) Poincare' section at these strobe times. Note that time increases as θ decreases in this figure. The plots show that as θ is adapted, the system passes in and out of chaotic and periodic behavior. Specifically, reading Figure 2(a) or (b) from left to right: (initially) chaotic $\rightarrow$ 3-periodic $\rightarrow$ chaotic $\rightarrow$ 2-periodic $\rightarrow$ 1-periodic $\rightarrow$ chaotic $\rightarrow$ 3-periodic $\rightarrow$ (finally) 1-periodic. Despite this complex behavior, the adaptation of θ continues to improve performance. In fact, as we shall shortly demonstrate, the adaptive parameter asymptotically approaches a small neighborhood of the *constant* value of θ which minimizes the average of $(x-r)^2$. This is precisely the desired property of the so-called gradient algorithm (6).

Figures 3(a)-3(k) show samples of the system state $(\theta, x, \dot{x})$ from four perspectives:

(1)***upper left***: 5 periods of phase plane $(\dot{x}, x)$.

(2)***upper right***: 5 periods of of $(\theta, x, \dot{x})$ vs. t.

(3)***lower right***: A crude spectral decomposition of $x(t)$ over 5 periods using the discrete Fourier transform,

$$X(\omega) = \frac{1}{N}\sum_{k=0}^{N-1} x(kT)\exp j\omega kT$$

with $T = 2\pi/200$ from (7), $N = 5(2\pi)/T + 1 = 1001$, and $\omega \in \{.05k : k = 0, 1, \ldots, 100\}$.

[2] Simulations and reprints of some of the results in [Ueda, 1980] can be found in many recent texts, *e.g.* , Thompson and Stewart(1986), Moon(1988).

(4)*lower left*: An (x,θ)-Poincare' section over 300 periods, the last 5 periods being those in the above plots. Observe that time t flows in the direction that θ deceases.

Comparison of the initial chaotic phase plot in Fig. 3(a) with the final periodic phase plot in Fig. 3(k) shows a significant improvement in performance as exhibited by the spectral plots.

4 Averaging Analysis

In this section we provide an analysis of the simulation results using the method of averaging. Following the approach described in Anderson *et al.*(1986), let $\bar{x}(t,\theta)$ denote the *frozen parameter state* corresponding to the adaptive nonlinear system (5)-(6) . That is, for constant θ, $\bar{x}(t,\theta)$ satisfies the forced Duffing system:

$$\ddot{\bar{x}} + k\dot{\bar{x}} + \bar{x}^3 = \theta A \cos t \tag{8}$$

Then, the "averaged parameter system" is defined as solutions of the autonomous system

$$\dot{\theta} = \gamma f_{\rm av}(\theta) \tag{9}$$

where for constant θ,

$$f_{\rm av}(\theta) = {\rm avg}\,\{r(\cdot)[r(\cdot) - \bar{x}(\cdot,\theta)]\} \tag{10}$$

with ${\rm avg}\,\{\cdot\}$ denoting the averaging operation

$${\rm avg}\,\{x(\cdot)\} = \lim_{T\to\infty} \frac{1}{T}\int_0^T x(t)\,dt \tag{11}$$

The method of averaging tells us (roughly) that for all small $\gamma > 0$, there exist solutions $\theta(t)$ of the adaptive system (5)-(6) which are within order-γ of equilibria of the averaged system (9) and which inherit the same stability type and approximately the same region of attraction.

To apply this to the simulation example recall that $r(t) = A\cos t$ with $A = 0.1$. Hence,

$$f_{\rm av}(\theta) = \frac{A}{2}[A - a(\theta)] \tag{12}$$

where $a(\theta)$ is defined for constant θ by

$$a(\theta) = 2{\rm avg}\,\{\bar{x}(\cdot,\theta)\cos(\cdot)\} \tag{13}$$

Thus, $a(\theta)$ is essentially a Fourier series coefficient corresponding to the 1-periodic component of the frozen parameter solution $\bar{x}(t,\theta)$.

To determine $a(\theta)$, consider the case where $\bar{x}(t,\theta)$ is well approximated by the pure harmonic

$$\bar{x}(t,\theta) = a(\theta)\cos t + b(\theta)\sin t$$

Substituting into (8), equating coefficients of $\cos t, \sin t$, and neglecting higher harmonics gives:

$$\begin{aligned} \theta A &= kb - (1 - \tfrac{3}{4}c^2)a \\ 0 &= ka + (1 - \tfrac{3}{4}c^2)b \\ c^2 &= a^2 + b^2 \end{aligned}$$

These formulae can be found in many texts, *e.g.* , [pg. 29, Hayashi(1964)]. A more useful form in our case is to parametrize a, b, θ in terms of c, the magnitude of the harmonic response. Thus,

$$\begin{aligned} a &= -c(1 - \tfrac{3}{4}c^2)/\sqrt{k^2 + (1 - \tfrac{3}{4}c^2)^2} \\ b &= kc/\sqrt{k^2 + (1 - \tfrac{3}{4}c^2)^2} \\ \theta &= (c/a)\sqrt{k^2 + (1 - \tfrac{3}{4}c^2)^2} \end{aligned} \tag{14}$$

Substitution into (12) gives,

$$f_{\rm av}(\theta) = \frac{A}{2}\left(A + \frac{c(1 - \frac{3}{4}c^2)}{\sqrt{k^2 + (1 - \frac{3}{4}c^2)^2}}\right) \tag{15}$$

Recall that the adaptive algorithm is designed to approximately minimize

$$V(\theta) = {\rm avg}\,\{(r - \bar{x})^2\} \tag{16}$$

Using (14), we also have

$$V(\theta) = \frac{1}{2}\left(a^2 + c^2 + \frac{2ca(1 - \frac{3}{4}c^2)}{\sqrt{k^2 + (1 - \frac{3}{4}c^2)^2}}\right) \tag{17}$$

Figure 4(a)-(b) shows plots of $(\gamma f_{\rm av}, \theta, V)$ vs. c on different scales. The equilibrium of the averaged system, $\bar{\theta}$, satisfies $f_{\rm av}(\bar{\theta}) = 0$. The expanded scale in Figure 4(b) reveals that $(\bar{\theta}, \bar{c}) = (.5878, 1.157)$. These predicted values are in close agreement with the simulation results, *i.e.* , from Figure 3(k), $(\bar{\theta}, \bar{c})_{\rm sim} \approx (.577, 1.25)$. Note that $\gamma f_{\rm av}$ is identical to $d\theta/dt$ in the averaged system (9). Values from the simulation are in general agreement with the predicted values in Figure 4:

$\bar{c}_{\rm sim}$	2.30	1.76	1.45	1.18
$\bar{\theta}_{\rm sim}$	-.0032	-.0036	-.0031	.0000
$\gamma f_{\rm av}$	-.0056	-.0038	-.0032	.0000

Figure 4(c) reveals that the equilibrium of the averaged system is stable because $df_{\rm av}/d\theta$ is strictly negative (although small) at the equilibrium. For comparison to the optimum, Figure 4(d) shows a plot of V vs. θ. Observe that $V(\bar{\theta}) = .66$ whereas the optimum, which occurs at $\theta_{\rm opt} = 1.9$, gives $V(\theta_{\rm opt}) = .62$. Hence, the equilibrium of the averaged system is close to the optimum, which implies that the simple gradient adaptation rule is well approximating the true gradient.

Figure 4 also reveals that the equilibrium has a large region of attraction, namely, for $c \in [1.1, 2.4]$ or equivalently $\theta \in [.55, 80]$. One can not immediately conclude that the adaptive system inherits this region of attraction because we have only examined the averaged system corresponding to an almost pure harmonic solution (14). Super- and sub-harmonic responses would in principal have to also be evaluated, and such formulae exist, *e.g.* , [Hayashi(1964)]. However, the spectral plots in Figures 3(a)-(k) show that in most instances the harmonic response tends to dominate. This lends credence to the conjecture that the adaptive system has a region of attraction which is well approximated by the region of attraction of the averaged system corresponding to the harmonic frozen parameter system solution (14). Again, comparison of predicted values with the simulation data points in Figure 4(a) tend to support this claim. The spectral plots also show that the chaotic behavior can be viewed to some extent as "noise" corrupting the harmonic "signal".

5 Concluding Remarks

The simulation results are encouraging and support the use of a simply constructed adaptive control to minimize the potentially deleterious effects of uncertain unmodeled nonlinearities. The method of averaging is shown to provide a good qualitative prediction of the system behavior despite the presence of chaotic and multi- periodic phenomena.

References

B.D.O. Anderson, R.R. Bitmead, C.R. Johnson, Jr., P.V. Kokotovic, R.L. Kosut, I.M.Y. Mareels, L. Praly, and B.D. Riedle, (1986),*Stability of Adaptive Systems: Passivity and Averaging Analysis*, MIT Press, 1986.

K.J. Åström and B. Wittenmark, *Adaptive Control*, Addison-Wesley, 1989.

B. Cyr, B.D. Riedle, and P.V.Kokotovic (1983), "Hopf bifurcation in an adaptive system with unmodelled dynamics," *Proc. IFAC Workshop on Adaptive Systems*, San Francisco, CA.

C. Hayashi, *Nonlinear Oscillations in Physical Systems*, McGraw-Hill, 1964.

I.M.Y. Mareels and R.R. Bitmead (1986), "Nonlinear dynamics in adaptive control: chatic and periodic stabilization," *Automatica*, vol. 22, pp.641-655.

I.M.Y. Mareels and R.R. Bitmead (1988), "Bifurcation effects in robust adaptive control," IEEE Trans. on Circuits and Systems, vol. 35, no. 7, pp. 835-841, July 1988.

F. Moon, *Chaotic Vibrations. An Introduction for Applied Scientists and Engineers*, Wiley, 1987.

B.D.Riedle and P.V.Kokotovic (1984), "Bifurcating equilibria in a simple adaptive system: simulation evidence," Proc. 1984 ACC, pp.238-240, San Francisco, CA.

F.M.A. Salam and S. Bai (1988), "Complicated dynamics of a prototype continuous-time adaptive control system," *IEEE Trans. on Circuits and Systems*, vol.35, no.7, pp. 842-849, July 1988.

S. Sastry and M. Bodson, *Adaptive Control: Stability, Convergence, and Robustness*, Prentice-Hall, 1989.

J.M.T. Thompson and H.B. Stewart, *Nonlinear Dynamics and Chaos*, Wiley, 1986.

Y. Ueda (1980), "Steady motions exhibited by Duffing's equation: a picture book of regular and chaotic motions," *New Approaches to Nonlinear Problems in Dynamics*, P.J. Holmes (ed.), pp. 311-322, SIAM.

B.E. Ydstie (1986), "Bifurcations and complex dynamics in adaptive control systems," *Proc. 25th IEEE CDC*, pp.2232-2236, Athens Greece, Dec. 1986.

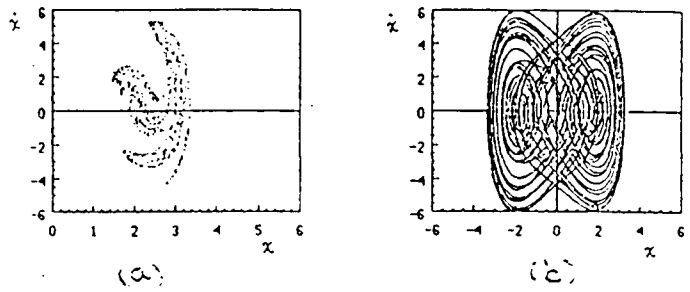

Figure 1: For $\ddot{x} + .05\dot{x} + x^3 = 7.5\cos t$, (a) Ueda's chaotic attractor at 900 2π-periodic strobes; (b) Time history over 50 periods.

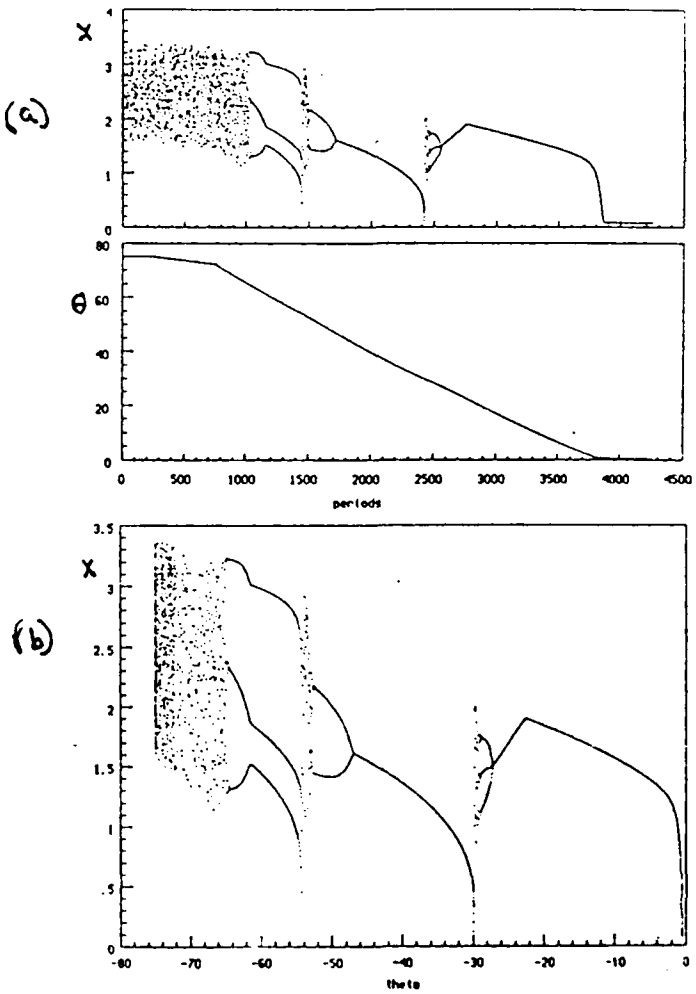

Figure 2: (a)(x, θ) vs. 1-period strobe times; (b) x vs. θ at 1-period strobe times.

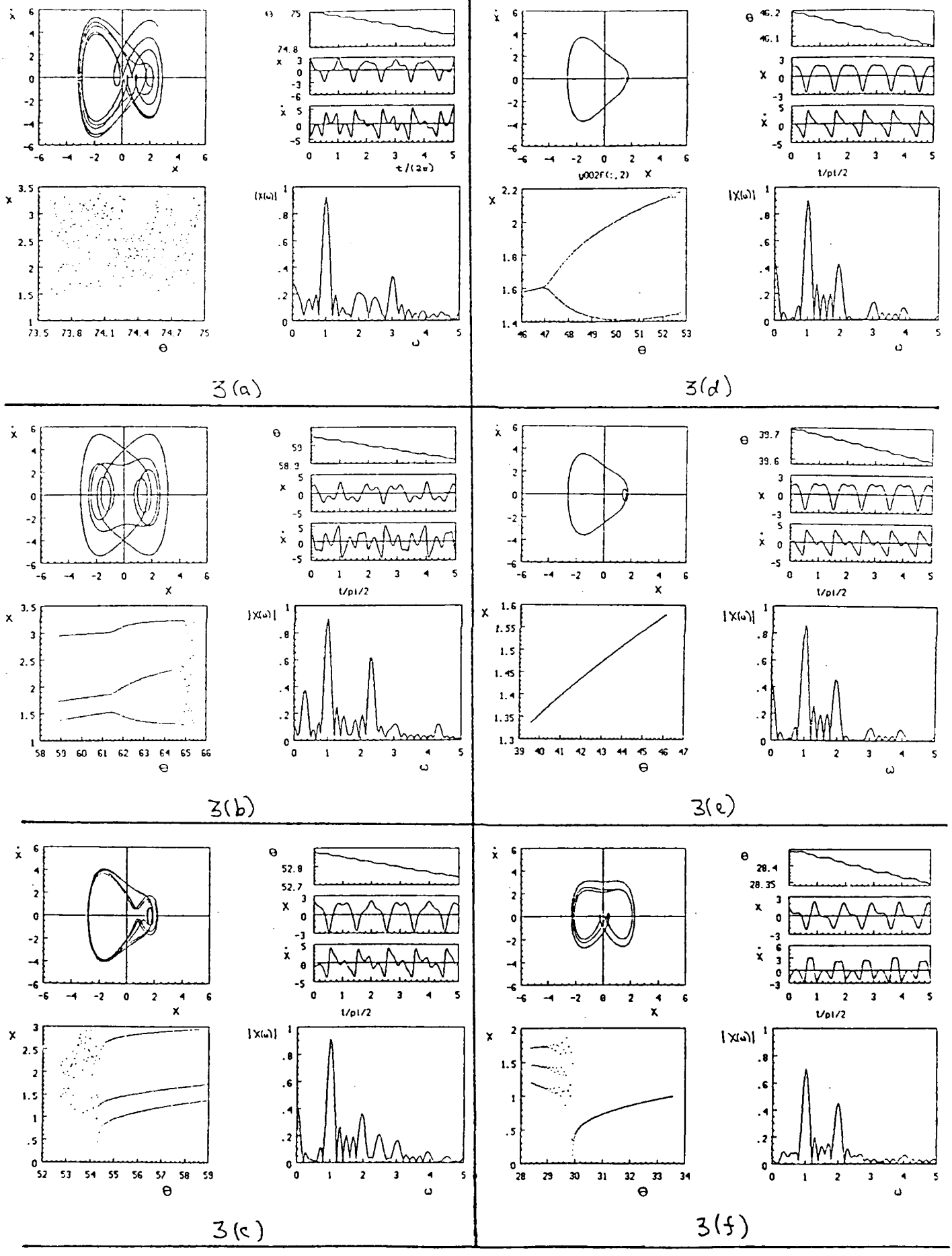

Figure 3: Samples of behavior during the simulation.

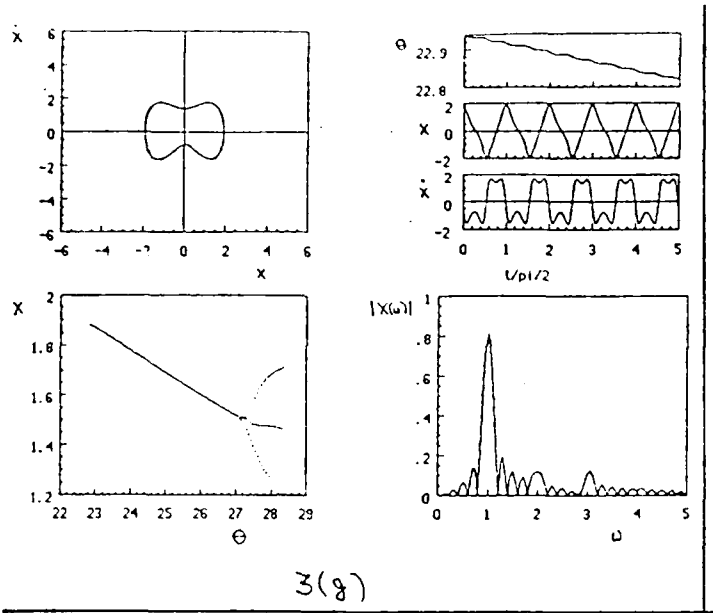

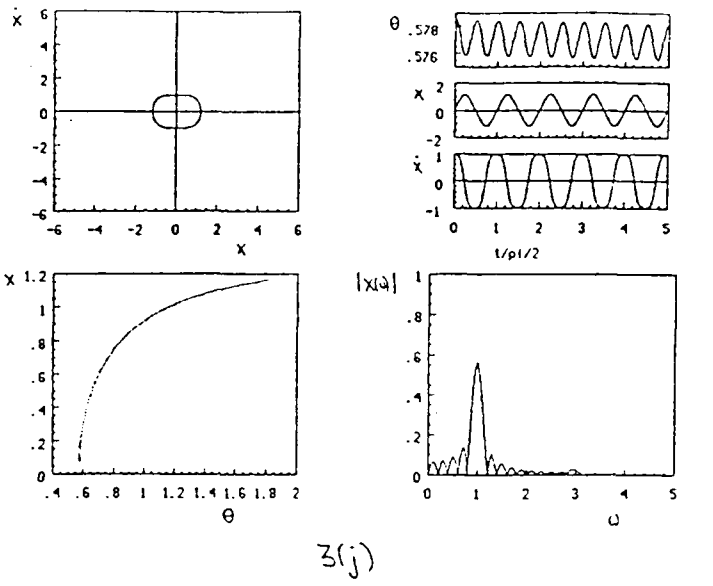

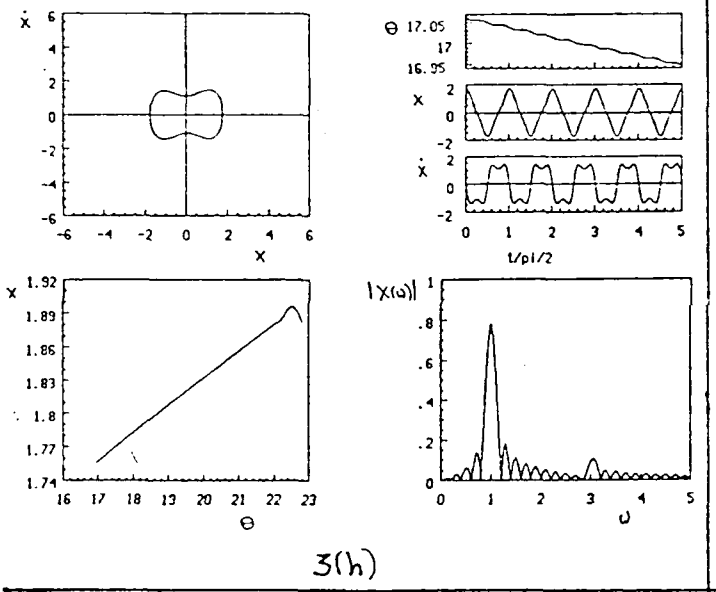

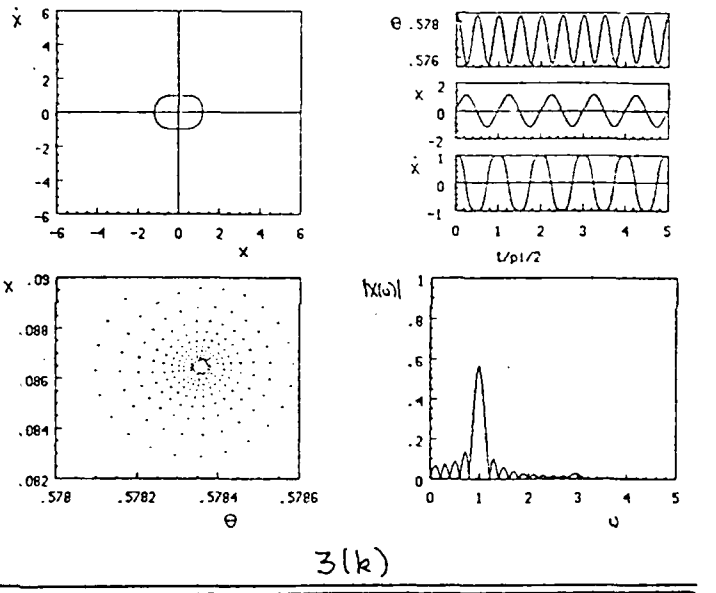

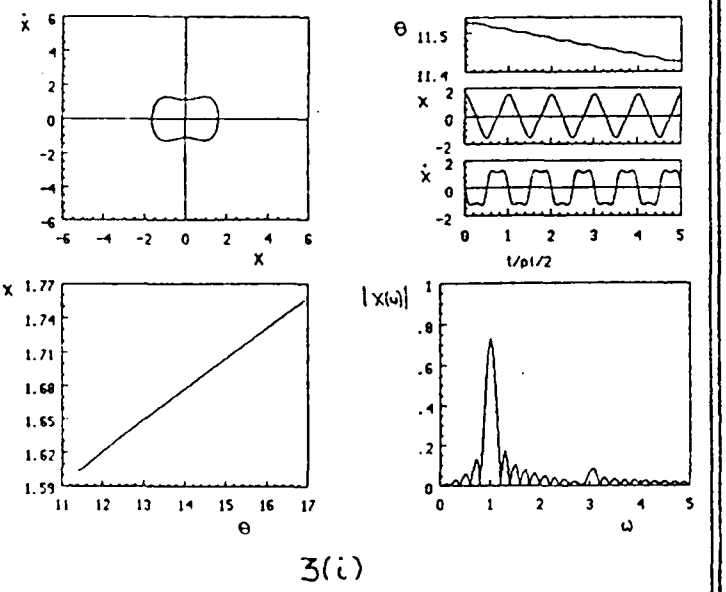

Figure 3: Samples of behavior during the simulation.

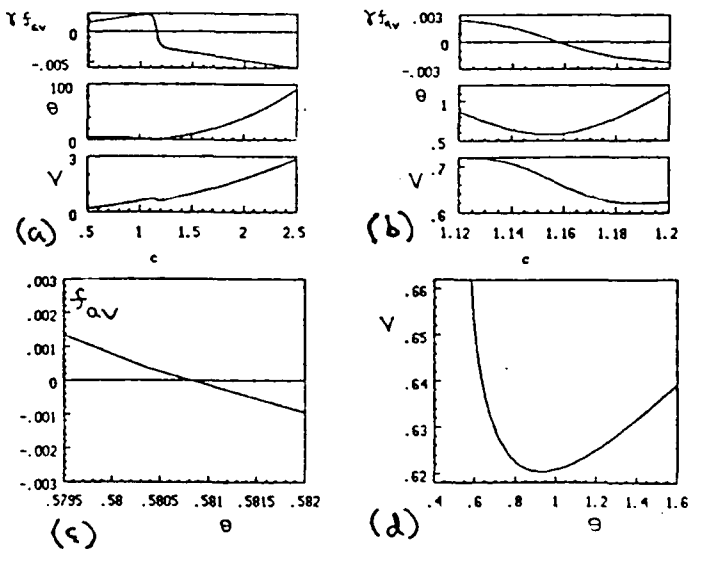

Figure 4: $(\gamma f_{av}, \theta, V)$ from (15),(16), and (18)

Closed-Loop Identification via the Fractional Representation: Experiment Design

Fred Hansen*
Sandia National Laboratories

Gene Franklin†
Information Systems Laboratory
Stanford University

Robert Kosut‡
Integrated Systems Inc.,
Stanford University

Abstract

An important aspect of system identification is the problem of experiment design. This paper uses a fractional representation approach to state and solve the closed-loop experiment design problem in terms of variables which are at the designer's disposal: the closed-loop inputs and the initial controller. Results of computer simulations are presented which compare optimal versus several non-optimal identification experiments

Introduction

The problem of system identification is to estimate the unknown parameters of a dynamical system or plant from measurements of systems input and output as shown in Figure 1a. In the figure, u is the measurable system input, y is the measurable system output and w is an unmeasurable system noise. Experiment design is the problem of choosing the experimental conditions (*e.g.* input signal u or sample time) to optimize the results of an identification experiment. In the case of open-loop operation, this is a well studied problem, see [1, 2] and *references therein*. Unfortunately, most actual identification experiments are conducted while the system is operating under closed-loop control (Figure 1b) and directly applying existing open-loop results to the closed-loop problem generally gives unsatisfactory results. Open-loop techniques can take into account the loop induced u-w correlation only at the expense of greatly increased complexity and generally yields a result in terms of the plant input u, a variable which is not at the designer's disposal. In this paper, the fractional representation [3, 4, 5] will be used to avoid the problem of the plant input and noise correlation and to obtain solutions directly in terms of the loop inputs and the initial controller, variables which are potentially at the designer's disposal.

*Supported by the Department of Energy Contract DE-AC04-76DP00789
†Supported by NSF Grant ECS-85-12041
‡Supported by AFOSR Contract F49620-89-C-0043DEF and NSF Grant ECS-86-05646

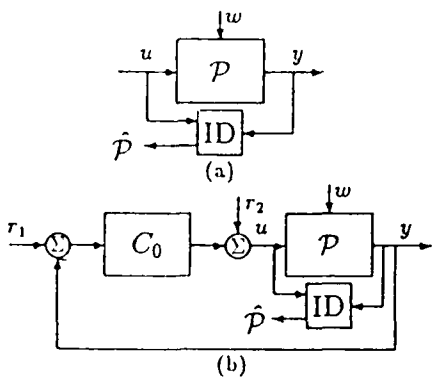

Figure 1: Block diagrams of open-loop and closed-loop system identification problems.

We assume that during the identification experiment the plant is in stable closed-loop control and that the initial stabilizing controller (C_0 in Figure 1b) is fixed and known. As an experiment design objective we use that proposed in [6]. It assumes that the estimated plant will be used to design a new controller and attempts to minimize errors in the closed-loop dynamics due to the new controller being designed for the estimated plant rather than the true plant. We present the optimal closed-loop input spectra which minimizes this objective subject to power constraints on the loop inputs, the plant input and/or the plant output. To our knowledge, this is the first time the closed-loop experiment design problem has been solved directly in terms of the loop inputs. We also derive the optimal initial controller (for use during the identification experiment) for the case of the a constraint on the power in the plant input and output. This result is a generalization of the results in [7].

(R, S) Parameterization

The results presented in this paper are derived by means of the fractional representation [3, 4, 5]. This theory represents both the plant and compensator as the ratio of stable coprime factors and has been used extensively in compensator design, for example [5, 8].

Let P_0 be a noise free plant and C_0 be any initial compensator which stabilizes P_0. Express P_0 as N_0/D_0 where N_0 and D_0 are stable and coprime (share no unstable zeros) and similarly express C_0 as the ratio of the stable coprime factors X_0/Y_0. Then all compensators which stabilize P can be shown [3, 4, 5] to be of the form

$$C_Q = \frac{X_0 + QD_0}{Y_0 - QN_0}, \tag{1}$$

where Q is stable. Conversely, C_Q, for any stable Q, will stabilize P.

By duality, all noise free plants which are stabilized by a given compensator can be similarly parameterized in terms of a stable parameter, say R, see [9]. In [10, 11] it is further shown that the noise dynamics of all plants stabilized by a given compensator can also be parameterized, by a stable, stably invertible parameter, S. These results are restated below.

The standard plant representation for identification is

$$\mathcal{P}: y = Gu + Hw. \tag{2}$$

where u, y and w are the plant input, output and noise respectively. G and H are the plant input/output and noise dynamics respectively. Assuming that $\mathcal{P}$ is stabilizable, then, without loss of generality, P can also be represented as

$$\mathcal{P}: Dy = Nu + Mw. \tag{3}$$

where N/D is a coprime factorization of G, and M is both stable and stably invertible. Define the triplet (D, N, M) to be the coprime factorization of the plant $\mathcal{P}$. Then, it can be shown [11] that a given plant $\mathcal{P}$ with coprime factorization (D, N, M) is stabilized by the compensator C_0 if and only if it can be expressed as

$$\mathcal{P}_{(R,S)} : y = G_R u + H_{(R,S)} w , \tag{4}$$

where

$$G_R = \frac{N_0 + RY_0}{D_0 - RX_0} = \frac{N}{D} , \tag{5}$$

$$H_{(R,S)} = \frac{S}{D_0 - RX_0} = \frac{M}{D} , \tag{6}$$

R is stable, S is stable and stably invertible, and X_0, Y_0, N_0, and D_0 are as defined previously. The parameters R and S are easily shown to be

$$R = \frac{D_0 N - N_0 D}{X_0 N + Y_0 D} \tag{7}$$

$$S = \frac{X_0 N_0 + Y_0 D_0}{X_0 N + Y_0 D} M . \tag{8}$$

Figure 2 shows a block diagram representation of $\mathcal{P}_{(R,S)}$.

Note that the parameters (R, S) form a subsystem within the plant: $\beta = R\alpha + Sw$. It is the properties of this (R, S) system which simplifies the closed-loop experiment design problem. These properties include:

1. R and S are the only unknowns in the plant/loop. The identification problem can be restated in terms of estimating (R, S) rather than (G, H).

2. The (R, S) system operates in open-loop. The gain from β to α is necessarily zero.

3. The input of the (R, S) system is $\alpha = X_0 r_1 + Y_0 r_2$ and is thus dependent only on the closed-loop inputs and the compensator. In particular, α is independent of both the true plant and the plant noise.

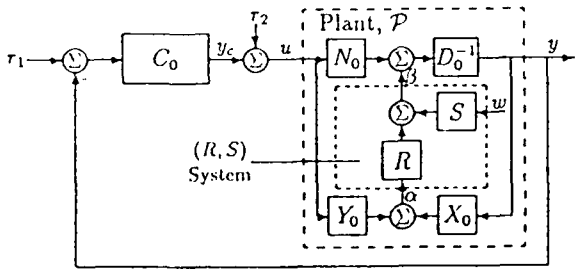

Figure 2: Closed-loop block diagram showing the unknown plant as a bridge centered on the (R, S) system.

These properties are easily verified using (4), (5), (6). Taken together, these properties allow the identification problem to be restated as one of estimating (R, S) from α and β rather than estimating (G, H) from u and y, thus transforming the closed-loop problem in an open-loop problem. In addition, property 3 indicates that α is dependent only on the closed-loop inputs and the initial compensator, quantities which are at the experiment designer's disposal. Therefore, any experiment design results for the (R, S) system which gives specifications on α will also solve the closed-loop experiment design problem.

Experiment Design Problem

As an experiment design objective, we use one suggested in [6] which is oriented specifically toward identification for the purposes of controller design. Assuming the estimated plant is used to design a new controller, this objective seeks to minimize errors in the closed-loop dynamics due to the fact that the controller was designed for the estimated plant rather than the true plant.

We make the following assumptions concerning the plant identification experiment.

1. The true plant, $\mathcal{P}_t$, is known to be a member of some known set Π. This set is such that there exists a robust controller which stabilizes all plants in Π.

2. During the identification experiment, the plant is controlled by a fixed initial stabilizing controller, C_0, which stabilizes all plants in Π. C_0 is assumed known.

3. After the identification experiment, the estimated plant, $\hat{\mathcal{P}}$, is used to design a new controller by some pre-defined design rule $\hat{C} = \mathcal{D}(\hat{\mathcal{P}})$.

The objective to be minimized is defined as

$$J_I = \mathcal{E}_w \int_{-\pi}^{\pi} |\Delta T_{yr_1}|^2 W_T d\omega \tag{9}$$

where $\mathcal{E}_w$ is the expectation operator with respect to the plant noise, W_T is a frequency-dependent weighting function, and ΔT_{yr_1} is the error in the closed-loop transfer function from r_1 to y (see Figure 2) as a result of $\hat{C}$ being designed for $\hat{\mathcal{P}}$ rather than $\mathcal{P}_t$. Thus

$$\Delta T_{yr_1} = \frac{G_t \hat{C}}{1 + G_t \hat{C}} - \frac{\hat{G}\hat{C}}{1 + \hat{G}\hat{C}} . \tag{10}$$

where G_t and $\hat{G}$ are the I/O dynamics of the true and estimated plants respectively and

We use a general power constraint on the signal α:

$$\int_{-\pi}^{\pi} \Phi_\alpha W_\alpha d\omega \leq K$$

where Φ_α is the power spectral density of α and W_α is a frequency-dependent weighting function.

Unfortunately, this objective-constraint pair cannot be solved directly. We therefore approximate the objective following the procedure described by Ljung in [2, 12]. First let $C_t = \mathcal{D}(\mathcal{P}_t)$ be the controller designed for the true plant. Let X_t/Y_t, (D_t, N_t, M_t) and $(\hat{D}, \hat{N}, \hat{M})$ be coprime factorizations of C_t, $\mathcal{P}_t$ and $\hat{\mathcal{P}}$ respectively. Finally, let (R_t, S_t) and $(\hat{R}, \hat{S})$ be the (R, S) parameterizations of $\mathcal{P}_t$ and $\hat{\mathcal{P}}$. Assuming that the plant estimate $\hat{\mathcal{P}}$ is "close" to the true plant $\mathcal{P}_t$ (in the sense that $\Delta R = R_t - \hat{R}$ is small) and the design rule $\mathcal{D}$ is continuous, then it is shown in [11] that $|\Delta T_{yr_1}|^2$ can be approximated to first order in $|\Delta R|$ by

$$|\Delta T_{yr_1}|^2 = W_R |\Delta R|^2 \tag{11}$$

where

$$W_R = \left| \frac{X_t Y_t (X_0 N_t + Y_0 D_t)^2}{(X_T N_t + Y_t D_t)^2 (X_0 N_0 + Y_0 D_0)} \right|^2 . \tag{12}$$

Thus, the J_I is approximately

$$J_I \cong \int_{-\pi}^{\pi} \mathcal{E}_w \{|\Delta R|^2\} W_R W_T d\omega .$$

Ljung shows in [2] that $\mathcal{E}_w |\Delta R|^2$ can be approximated asymptotically for large n, large N and small n/N by

$$\mathcal{E}_w |\Delta R|^2 \cong \frac{n}{N} \frac{|S_t|^2 \Phi_w}{\Phi_\alpha} \tag{13}$$

where n is the order of the plant model in the identification algorithm, N is the number of data points used in the identification and Φ_w and Φ_α are power spectral densities of w and α [12]. This approximation assumes that identification algorithm is a PEM (Prediction Error Method) type, that the (R_t, S_t) system is in open-loop and that the true model is in the model set (*i.e.* no unmodeled dynamics).

Collecting everything except Φ_α into a single objective weighting function, W_{obj}, the final design problem becomes:

$$\text{Minimize: } J_I = \int_{-\pi}^{\pi} \frac{W_{obj}}{\Phi_\alpha} d\omega \tag{14}$$

with respect to Φ_α and possibly C_0 subject to the constraint

$$\int_{-\pi}^{\pi} \Phi_\alpha W_\alpha(\omega) d\omega \leq K \tag{15}$$

where

$$W_{obj} = \frac{n}{N} |S_t|^2 \Phi_w W_R W_T. \tag{16}$$

Solutions to this design problem are discussed in the following section.

Optimal Designs

We consider two different design problems. In one, the initial controller is assumed fixed and we obtain the set of optimal closed-loop input signals. In the other, we find both the optimal initial controller and the closed-loop input signals. We first consider the constraint in more detail.

The Constraint

Often the loop inputs represent physical quantities which need to be constrained during the identification experiment. A constraint on α does not directly yield a constraint on r_1 and r_2 since the inverse map from α to r_1 and r_2 is not unique. However, if the power apportionment between r_1 and r_2 is determined *a priori* then (15) immediately becomes a constraint on the loop inputs.

For example, suppose that the loop is to be driven from r_1 only. Then, $\alpha = X_0 r_1$ (with $r_2 = 0$), and a general power constraint on r_1 of the form

$$\int_{-\pi}^{\pi} \Phi_{r_1} W_{r_1}(\omega) d\omega \leq K$$

is accomplished via (15) by using the weighting function

$$W_\alpha = \left| X_0^{-1} \right|^2 W_{r_1}. \tag{17}$$

Likewise, if only r_2 is to be used to drive the loop, the appropriate choice of W_α in (15) is

$$W_\alpha = \left| Y_0^{-1} \right|^2 W_{r_2}. \tag{18}$$

Also, a constraint on the total power in the loop inputs is accomplished by setting

$$W_\alpha = \left| (\max\{X_0(\omega), Y_0(\omega)\})^{-1} \right|^2. \tag{19}$$

where it has been assumed that each input (r_1 or r_2) will be used only at those frequencies where it has the highest gain to the internal signal α. These weighting functions is listed in Table 1.

It is also common for the loop inputs to be non-physical numbers somewhere inside a feedback control program. In this case constraining the loop inputs has little meaning and it makes more sense to constrain the input and output of the plant itself. Denote that portion of u and y which is due only to the loop inputs as u_r and y_r, Then, by the proper choice of W_α, (15) can also be used to constrain the power in u_r and y_r. See [11] for details. These weighting function are also listed in Table 1.

Constraint	W_α
$\int_{-\pi}^{\pi} \Phi_{r_1} W_{r_1} d\omega \leq K$	$\lvert X_0^{-1} \rvert^2 W_{r_1}$
$\int_{-\pi}^{\pi} \Phi_{r_2} W_{r_2} d\omega \leq K$	$\lvert Y_0^{-1} \rvert^2 W_{r_2}$
Total input power	$\left\lvert (\max\{X_0, Y_0\})^{-1} \right\rvert^2$
$\int_{-\pi}^{\pi} \Phi_{y_r} W_{y_r} d\omega \leq K$	$\left\lvert \frac{N_t}{N_t X_0 + D_t Y_0} \right\rvert^2 W_{y_r}$
$\int_{-\pi}^{\pi} \Phi_{u_r} W_{u_r} d\omega \leq K$	$\left\lvert \frac{D_t}{N_t X_0 + D_t Y_0} \right\rvert^2 W_{y_r}$

Table 1: Several possible constraints which can be put in the form (15) and the corresponding W_α.

Loop Input Design

The problem of minimizing (14) with respect to Φ_α subject to (15) is a standard minimization problem which admits a closed form solution [2]. The solution is

$$\Phi_{\alpha,opt} = \gamma \sqrt{\frac{W_{obj}}{W_\alpha}}. \tag{20}$$

where γ is a scaling constant chosen so that equality is obtained in the constraint. The optimal spectra for the closed-loop inputs r_1 and r_2 must therefore be such that

$$\Phi_{\alpha,opt} = |X_0|^2 \Phi_{r_1,opt} + |Y_0|^2 \Phi_{r_2,opt}. \tag{21}$$

Thus, the optimal closed-loop inputs are characterized not by a single pair of spectra for r_1 and r_2, but rather by the set of non-negative definite solutions to (21). This solution set can be shown [11] to be independent of the particular choice of the nominal plant $\mathcal{P}_0$, and coprime factorizations for $\mathcal{P}_0$ (N_0/D_0), for $\mathcal{P}_t$ (D_t, N_t, M_t), for C_t (X_t/Y_t) and for C_0 (X_0/Y_0).

The solution given by (20) and (21) has the disadvantage that it depends on the true plant through W_{obj} and, in some cases, W_α. Though this problem is shared by most other experiment design solutions in the literature, it severely limits the solution's practical utility. To address this, we propose to restate the original design problem in terms of an average over all possible plants. The plant has been assumed a member of a known set Π. We further assume that the true plant is a random variable with a known distribution within that set. The averaged design problem can then be stated as:

$$\text{Minimize } J_{I,ave} = \mathcal{E}_{\mathcal{P}_t} \int_{-\pi}^{\pi} \frac{W_{obj}}{\Phi_\alpha} d\omega \tag{22}$$

subject to the average constraint

$$\mathcal{E}_{\mathcal{P}_t} \int_{-\pi}^{\pi} \Phi_\alpha W_\alpha d\omega \leq K, \tag{23}$$

where $\mathcal{E}_{\mathcal{P}_t}$ is the expectation operator over all possible true plants. Both expectations are assumed finite. Therefore the expectation and integration operator can be exchanged and the solution is easily shown to be

$$\Phi_{\alpha,opt-ave} = \gamma \sqrt{\frac{\mathcal{E}_{\mathcal{P}_t} W_{obj}}{\mathcal{E}_{\mathcal{P}_t} W_\alpha}}. \tag{24}$$

In the rest of the paper, this spectrum will be referred to as the "optimal averaged spectrum". Note that this is not simply the result of averaging the optimal spectrum over Π.

Controller Design

The previous section considered the problem of finding the optimal closed-loop input signals given a fixed initial controller. In this section we will consider the problem of finding both the optimal closed input signal and the optimal initial controller. The special case considered is that of the design constraint being of "LQG-type" on the power of the plant input and output. In particular we will

$$\text{Minimize} \quad J_I = \int_{-\pi}^{\pi} \frac{W_{\text{obj}}}{\Phi_\alpha} d\omega \tag{25}$$

with respect to both C_0 and Φ_α, subject to the constraint

$$\int_{-\pi}^{\pi} (a^2 \Phi_u + b^2 \Phi_y) d\omega \leq K . \tag{26}$$

First note that since the loop is linear, the constraint can be restated as

$$\int_{-\pi}^{\pi} (a^2 \Phi_{u_r} + b^2 \Phi_{y_r}) d\omega \leq K - \int_{-\pi}^{\pi} (a^2 \Phi_{u_w} + b^2 \Phi_{y_w}) d\omega = K_r . \tag{27}$$

where K_r is defined as shown. As in before, u_r is that component of u due entirely to the closed loop inputs and u_w is that component of u due to the plant noise w, likewise with y_r and y_w. From Table 1, this can be expressed in the form of (15) with

$$W_\alpha = \frac{a^2 |D_t|^2 + b^2 |N_t|^2}{|X_0 N_t + Y_0 D_t|^2} . \tag{28}$$

From the previous section, the optimal Φ_α for a given C_0 is

$$\Phi_{\alpha,\text{opt}|C_0} = \gamma \sqrt{\frac{W_{\text{obj}}}{W_\alpha}} \tag{29}$$

where γ is chosen such that the equality is achieved in the constraint. Thus γ is

$$\gamma = \frac{K_r}{\int_{-\pi}^{\pi} \sqrt{W_{\text{obj}} W_\alpha} d\omega} . \tag{30}$$

which implies that the minimum J_I for any given C_0 is

$$J_{I,\min|C_0} = \frac{\left(\int_{-\pi}^{\pi} \sqrt{W_{\text{obj}} W_\alpha} d\omega \right)^2}{K_r} . \tag{31}$$

Minimizing this with respect to C_0 will yield the optimal initial compensator for the identification experiment. Using (16), (12) and (28), $W_{\text{obj}} W_\alpha$ becomes

$$W_{\text{obj}} W_\alpha = \frac{n}{N} \Phi_w W_T (a^2 |D_t|^2 + b^2 |N_t|^2) \left| \frac{M_t X_t Y_t}{(X_t N_t + Y_t D_t)^2} \right|^2 .$$

The important point is that this product is independent of the initial compensator C_0. Thus, the only term in the cost $J_{I,\min|C_0}$ which is a function of C_0 is K_r and $J_{I,\min|C_0}$ will achieve a minimum when K_r achieves its maximum. K_r is maximized when

$$J_{\text{LQG}} = \int_{-\pi}^{\pi} (a^2 \Phi_{u_w} + b^2 \Phi_{y_w}) d\omega \tag{32}$$

is minimized (see (27)) which is the precisely the LQG problem. Therefore, the optimal controller to use during the during the identification experiment when the design constraint is of "LQG-type" is the associated LQG controller. The optimal loop input spectrum is given by (29). Note that this result is independent of the weighting function in the objective, W_T, or the new-compensator design rule $\mathcal{D}$.

This result contains, as special cases, two previously published results by Ljung and others [2, 6, 7] on optimal controllers for closed-loop identification and shows them to be the extremes in a continuum of such design problems. In [2, 6] the authors show that if the constraint is placed on u alone then open-loop operation is optimal for plant identification, assuming that the plant is stable. By a similar analysis it is shown in [7] that a plant output constraint implies a minimum variance controller is optimal, assuming that the plant is minimum phase. Both of these results are special cases of the solution presented here. If $a = 1$ and $b = 0$, the constraint is on u and minimizing J_{LQR} yields the "high cost of control" solution (open-loop operation when $\mathcal{P}$ is stable). If $a = 0$ and $b = 1$,the constraint is on y and the optimal C_0 is the "cheap control" solution, (the minimum variance controller when $\mathcal{P}$ is minimum phase). However, the solution presented here is valid if the plant is unstable or non-minimum phase and for the continuum of values of a and b between these two extremes.

The original constraint (26) specifies a maximum on the total power of u and y. The LQG controller, merely seeks to minimize the noise contribution toward this maximum leaving as much power as possible for the "signal" contribution of α. Thus this solution can be interpreted as using that C_0 which maximizes the signal-to-noise ratio in the signals u and y. This solution also has the implication that the initial controller is important only in the case where the constraint is small enough that the plant noise makes a significant contribution to K.

Simulations

To illustrate this experiment design technique we offer the following simulation examples. In these simulations, the plant is stabilized by an initial fixed controller and is identified from 500 input-output data samples. The final estimated plant is used to design a new compensator. The resulting closed-loop transfer functions are calculated for the loops containing the new compensator and the true plant $T_{\mathcal{P}_i}$, and the new compensator and the estimated plant, $T_{\hat{\mathcal{P}}}$. Finally, the simulated experimental objective is obtained by averaging the integral squared difference between $T_{\mathcal{P}_i}$ and $T_{\hat{\mathcal{P}}}$ over 100 independent simulations. Note that this is the original objective (9), not the approximation.

The set of plants we consider was first suggested in [13] as a benchmark problem for system identification, adaptive control and robust control. The continuous time model is

$$y = .9 \left(\frac{1}{s^2} - \frac{1}{s^2 + 2 w_r \xi s + w_r^2} \right) u \tag{33}$$

The unknown parameters in the system are w_r, the natural frequency, and ξ, the damping ratio, and are assumed to be in the intervals,

$$\begin{aligned} 1 \text{ Hz} \leq \quad & w_r/2\pi \quad \leq 2 \text{ Hz} \\ .02 \leq \quad & \xi \quad \leq .1 \end{aligned} \tag{34}$$

These uncertainties comprise the set Π. When necessary we assume w_r and ξ are uniformly distributed. We simulated two particular plants in this set; $\mathcal{P}_1$ with $(w_r, \xi) = (1\text{Hz}, 0.1)$ and $\mathcal{P}_2$with $(w_r, \xi) = (2\text{Hz}, 0.02)$.

This plant was transformed into a discrete plant assuming a zero-order-hold and a sampling rate of 20 Hz. No noise model was included [13]. We assume the full plant dynamics (input/output and noise) are of the form:

$$\begin{aligned} \mathcal{P} \quad : \quad & (1 + a_1 z^{-1} + a_2 z^{-2} + a_3 z^{-3} + a_4 z^{-4}) y = \\ & (b_1 z^{-1} + b_2 z^{-2} + b_3 z^{-3} + b_4 z^{-4}) u + w \end{aligned} \tag{35}$$

where w is white Gaussian noise. All eight coefficients are estimated. The initial controller is

$$C_0 = \frac{1 - 2.69z^{-1} + 2.53z^{-2} - .841z^{-3}}{1 - .725z^{-1} - .175z^{-2} - .00925z^{-3}}. \qquad (36)$$

which stabilizes all plants within the uncertainty (34). With this controller the closed-loop has essentially the same resonance as the plant. This resonance will have a noticeable impact on the final experiment designs.

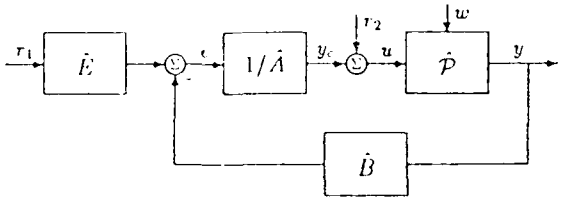

Figure 3: Final control system in STR configuration

The estimated plant is used to design a new controller in the configuration shown in Figure 3. Letting $\hat{\omega}_r$ be the estimated plant's natural frequency, $\hat{A}$ and $\hat{B}$ are chosen so that:

a) the resonant poles are radially projected inwards by a factor of .95 (the "control" poles) and .85 (the "estimator" poles), and

b) the double integrator poles are moved to a natural frequency of $(.3 + .3\hat{\omega}_r)$ with a damping ratio of .85 ("control" poles) and a natural frequency of $(1 + \hat{\omega}_r)$ with a damping ratio of .9 ("estimator" poles).

$\hat{E}$ is then selected so that the four selectable closed-loop zeros coincide with the "estimator" poles specified above. This choice makes the overall control design equivalent to a state-estimator/state-variable-feedback controller. This particular dependence on $\hat{\omega}_r$ was chosen to obtain a faster closed-loop with the faster plants (those with higher resonant frequencies).

Experiments are designed to minimize

$$J_I = \int_{-\pi}^{\pi} |\Delta T_{yr_1}|^2 d\omega.$$

This new controller is slightly more general than that considered earlier due to the presence of the pre-compensator. By similar arguments this objective can be approximated by

$$J_I \cong \int_{-\pi}^{\pi} \frac{W_{obj}}{\Phi_\alpha} d\omega,$$

where W_{obj} is

$$W_{obj} = \frac{n}{N}\lambda|S_I|^2 \left| \frac{B_I A_I (X_0 N_I + Y_0 D_I)^2}{(B_I N_I + A_I D_I)^2 (X_0 N_0 + Y_0 D_0)} \right|^2 \left| \frac{E_I}{B_I} \right|^2 \qquad (37)$$

and A_I, B_I, and E_I comprise the new compensator designed for the true plant. All other notation is consistent with that used in Section 2 with B_I and A_I corresponding to X_I and Y_I respectively.

The first set of results we present are for the case where a power constraint is placed on the loop input r_2. Note that this constraint is one which can not be addressed by previously published experiment design techniques. Figure 4 shows the four input spectra used in the simulations. It includes the optimal

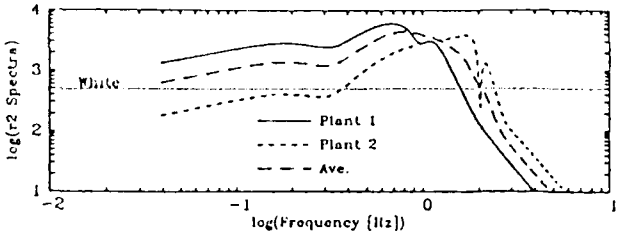

Figure 4: Optimal r_2 spectra assuming the true plant to be $\mathcal{P}_1$ and $\mathcal{P}_2$, the averaged optimal spectrum and a white spectrum. Optimal spectra calculated for a power constraint on r_2.

spectra assuming the true plant to be $\mathcal{P}_1$ and $\mathcal{P}_2$, the optimal averaged spectrum and a white spectrum, all of unity power. Note how the optimal spectrum for $\mathcal{P}_2$ notches out the plant's resonant frequency. Recall that when C_0 is used, the plant and loop have the same resonance. Therefore, if $\mathcal{P}_2$ is the true plant, the gain from r_2 to both u and y will be large at 2 Hz; little power is required at that frequency to excite the plant, thus the notch.

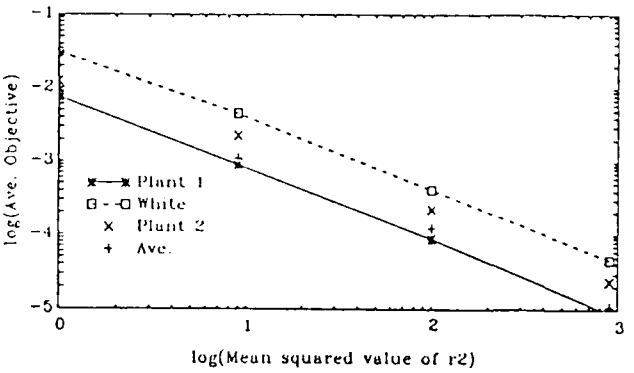

Figure 5: Simulation results obtained when true plant is $\mathcal{P}_1$ and loop is driven by spectra shown in Figure 4.

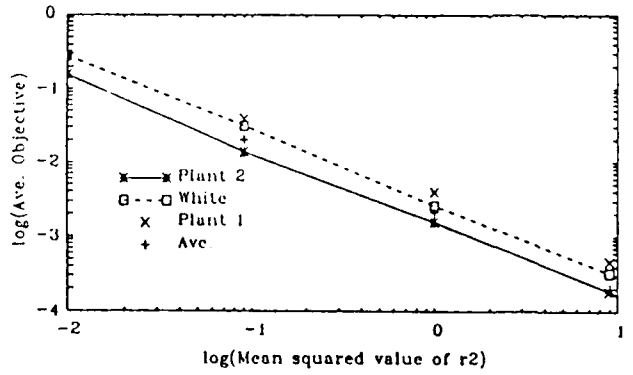

Figure 6: Simulation results obtained when true plant is $\mathcal{P}_2$ and loop is driven by spectra shown in Figure 4.

Two parallel sets of simulators were run, one with the true plant being $\mathcal{P}_1$ and the other with $\mathcal{P}_2$. Figures 5 and 6 show the average experimental objective versus input power at r_2 for each of the four spectra in Figure 4. In each simulation the plant was also driven by a white noise at w of power $\lambda = 10^{-4}$.

In both sets of simulations, the optimal spectra for the true plant provides the best plant identification, a factor of 3 better than a white input is $\mathcal{P}_1$ is the true plant and a factor 2 better if $\mathcal{P}_2$ is the true plant. Note also that if $\mathcal{P}_2$ is the true plant, using a

spectrum designed to $\mathcal{P}_1$ is worse than simply a white loop input. However, the optimal averaged input provides a superior plant identification than either a white input or an input designed for the "wrong" plant and nearly as good an identification as the optimal input spectrum.

In a final set of simulations we tested the optimal initial controller result presented earlier. In this example we choose the constraint to be

$$\int_{-\pi}^{\pi} (.5\Phi_u + .5\Phi_y)d\omega \leq K$$

for some K. The optimal initial controller is the LQG controller designed to minimize the control cost

$$\int_{-\pi}^{\pi} (.5\Phi_{u_\omega} + .5\Phi_{y_\omega})d\omega$$

where u_ω and y_ω are those portions of u and y, respectively, due to the plant noise alone. To test this result, we performed simulated identification experiments using five different LQG controllers designed to minimize the control cost

$$\int_{-\pi}^{\pi} (\rho\Phi_{u_\omega} + (1-\rho)\Phi_{y_\omega})d\omega$$

for ρ = 0.99, 0.9, 0.5, 0.1 and 0.01, each assuming the $\mathcal{P}_2$ was the true plant. As a sixth alternative, experiments were also simulated using the initial robust controller presented earlier in this section. For the purposes of this example the LQG controllers will be referred to as $C_{0,\rho}$ and the robust controller will be denoted $C_{0,rob}$.

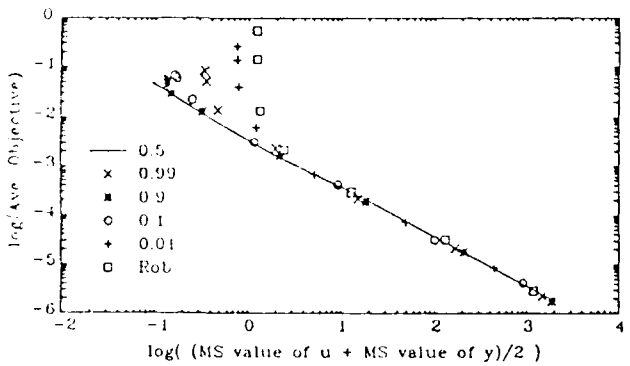

Figure 7: Simulation for the initial controllers $C_{0,99}$ through $C_{0,01}$ and $C_{0,rob}$. In all simulations the true plant is $\mathcal{P}_2$.

Figure 7 shows the results of simulations using each of these six initial controllers. In all cases, $\mathcal{P}_2$ was the true plant. As before, each data point is the average of 100 independent simulations. These simulations confirm that $C_{0,.5}$ is the best initial controller, providing the lowest average objective over 4 orders of magnitude in both the constraint and the objective. Just as importantly, these results confirm that the initial controller is important only if the constraint is sufficiently small that the plant noise is a significant component of the plant input and output.

Conclusion

The problem of system identification experiment design in which the system to be identified is operating in a stable closed loop has been addressed. We have shown how to minimize the objective proposed by Yuan and Ljung [6] subject to power constraints on the closed-loop inputs, the plant input and/or the plant output. In addition to being more general than other solutions, our solution has the unique feature that it yields specifications on variables which are at the designer's disposal, *i.e.* the closed-loop inputs and the initial compensator used during the experiment. Previous solutions yield specifications on the plant input, a variable which not at the designer's disposal. The solution for the optimal initial compensator contains two previously published results as special cases and shows them to be the extremes of a continuum of such solutions. We also presented simulation results which demonstrate the use of our method.

In this paper, we have not addressed the important problem of unmodeled dynamics. However, we believe that this method offers advantages here as well. For example, the weighting function W_T can be selected to de-emphasize those frequencies were the unmodeled dynamics are dominate. Furthermore, the fact that the (R,S) system is necessarily stable simplifies the techniques for on-line uncertainty estimation in [14] and broadens the techniques in [15, 16] to be applicable to any system operating in a stable closed-loop.

References

[1] R. K. Mehra. Choice of input signals. In *Trends and Progress in System Identification*. Pergamon Press, Elmsford, New York, 1981.

[2] L. Ljung. *System Identification, Theory for the User*. Prentice-Hall, 1987.

[3] D. C. Youla, J. J. Bongiorno, and H. A. Jabr. Modern Wiener-Hopf design of optimal controllers, part i: The single-input case. *IEEE Trans. on Auto. Control*, AC-21:3-14, Feb 1976.

[4] C. A. Desoer, R. W. Liu, J. Murray, and R. Sacks. Feedback system design: The fractional representation approach to analysis and synthesis. *IEEE Trans. Auto. Control*, AC-25:399-412, June 1980.

[5] M. Vidyasagar. *Control System Synthesis: A Factorization Approach*. MIT Press, Cambridge Mass, 1985.

[6] Z. Yuan and L. Ljung. Unprejudiced optimal open loop design for identification of transfer functions. *Automatica*, 21(6):697-708, 1985.

[7] M. Gevers and L. Ljung. Benefits of feedback in experiment design. In 7th *IFAC Symposium on Identification and System Parameter Estimation*, pages 909-914, York, UK, July 1985. IFAC/IFORS.

[8] S. P. Boyd, V. Balakrishnan, C. H. Barratt, N. M. Kraishi, X. Li, D. G. Meyer, and S. A. Norman. A new CAD method and associated architectures for linear controllers. *IEEE Trans. on Auto. Control*, AC-33(3):268-283, 1988.

[9] Q. Haung and R. W. Liu. A necessary and sufficient condition for stability of a perturbed system. *IEEE Trans. Auto. Control*, AC-32:337-340, April 1987.

[10] F. Hansen and G. Franklin. On a fractional representation approach to closed-loop experiment design. In *Proc. Joint Automatic Control Conf.*, pages 1319-1320, Atlanta, Ga, June 1988.

[11] F. Hansen. *A Fractional Representation Approach to Closed-loop System Identification and Experiment Design*. PhD thesis, Stanford University, Stanford, CA, March 1989.

[12] L. Ljung. Asymptotic variance expressions for identified black-box transfer function models. *IEEE Trans on Auto. Control*, AC-30(9):834-844, Sep 1985.

[13] C. R. Johnson, A. Foss, G. Franklin, R. Monopoli, and G. Stein. Toward development of a practical benchmark example for adaptive control. *Control Systems Magazine*, 1(4):25-28, Dec 1981.

[14] R. Kosut. Adaptive control via parameter set estimation. *Int. Journal of Adaptive Control and Signal Processing*, 2:371-399, 1989.

[15] B. Walberg. On model reduction in system identification. In *Proceedings of the 1986 American Control Conference*, pages 1260-1266, Seattle, Wa, June 1986.

[16] R. O. LaMaire, L. Lalavani, M. Athans, and G. Stein. A frequency estimator for use in adaptive control systems. In *Proceedings of the 1987 American Control Conference*, pages 238-244, Minneapolis, Minn., June 1987.